

Inhibition of Matrix Metalloproteinases by Hydroxamates Containing Heteroatom-Based Modifications of the P₁' Group

Madhusudhan R. Gowravaram,[†] Bruce E. Tomczuk,^{*,†} Jeffrey S. Johnson,[†] Daniel Delecki,[†] Ewell R. Cook,[†] Arup K. Ghose,[‡] Alan M. Mathiowetz,[‡] John C. Spurlino,[‡] Byron Rubin,[‡] Douglas L. Smith,[‡] Tricia Pulvino,[§] and Robert C. Wahl[§]

Departments of Medicinal Chemistry, Biophysics and Computational Chemistry, and Biochemistry, Sterling Winthrop Pharmaceuticals Research Division, 1250 South Collegeville Road, P.O. Box 5000, Collegeville, Pennsylvania 19426-0900

Received November 1, 1994[⊙]

In this study, structure-based drug design of matrix metalloproteinase inhibitors [human fibroblast collagenase (HFC), human fibroblast stromelysin (HFS), and human neutrophil collagenase (HNC)] was utilized in the development of potent hydroxamates which contain novel, heteroatom-based modifications of the P₁' group. A series containing a P₁' butyramide group resulted in a nanomolar potent and selective HNC inhibitor as well as a dual HFS/HNC inhibitor. Benzylic ethers with a four- or five-carbon methylene linker in the P₁' position also produced nanomolar potent HFS/HNC inhibition and micromolar potent HFC inhibition as expected. Surprisingly, the phenolic ethers of the same overall length as the benzylic ethers showed nanomolar potencies against HFC, as well as HFS and HNC. The potency profile of the phenolic ethers was optimized by structure-activity relationships of the phenolic group and the C-terminal amide. These inhibitors may help elucidate the *in vivo* roles of matrix metalloproteinases in normal and disease states.

Enzymes of the matrix metalloproteinase (MMP) family share several characteristics such as extracellular activity, presence of an essential zinc for catalysis, secretion as an inactive proenzyme, and modulation by macromolecular tissue inhibitors of metalloproteinases (TIMPs).¹ The members of this family, currently numbering 12, can be classified into three groups, such as the collagenases which cleave triple-helical interstitial collagen, the stromelysins which cleave mainly proteoglycans, and the gelatinases which cleave denatured collagen, elastin, and types IV and V collagen. The cleavage and degradation of collagen and proteoglycan, two major components of connective tissue, signify a role for the MMPs in extracellular matrix remodeling and degradation.

The role of the MMPs in normal and disease states is not well understood. Under normal circumstances, the activity of the MMPs is tightly modulated by latency and endogenous inhibitors, such as α_2 -macroglobulin and TIMPs. A certain amount of activated MMPs may be necessary for normal matrix remodeling and maintenance. However, excessive MMP synthesis and release would lead to connective tissue degradation and ultimate destruction. As evidence, increased levels of these enzymes have been observed in the cartilage and synovium of patients with rheumatoid and osteoarthritis and correlate to the severity of the disease.² Other MMPs such as the gelatinases have been implicated in the breakdown of basement membranes. These enzymes have been found at elevated levels in tumor cell lines and may be responsible for the metastases of tumors.³

Excessive MMP activity has also been associated with periodontal disease.⁴ Other conditions where MMPs may be involved include corneal ulceration resulting from infection or chemical damage,⁵ multiple sclerosis,⁶ and atherosclerosis and coronary thrombosis,⁷ aortic aneurysms,⁸ and skin lesions in dystrophic epidermolysis bullosa.^{9,10} Stromelysin has been demonstrated to degrade α_1 -proteinase inhibitor (α_1 -PI), an endogenous inhibitor of elastase, a destructive enzyme implicated in chronic lung diseases such as emphysema.¹¹ Thus, an inhibitor of stromelysin may potentiate the elastase inhibitory effects of α_1 -PI.

The development of specific bioavailable inhibitors of the MMPs would aid in delineating the role of these enzymes in normal and disease states. There are several known classes of inhibitors of MMPs, such as hydroxamates, thiols, phosphorus-types (phosphinate, phosphonate, and phosphoramidate), and *N*-carboxyalkyls, which have been extensively reviewed.¹²⁻¹⁶ The common structural features include a moiety capable of chelating to the essential zinc metal found at the catalytic site and a peptidic fragment capable of binding to a subset of the specificity pockets of the enzymes, usually on the P' side. Generally, the P₁' side chain has an isobutyl group as depicted in 1 (Table 1). The P' side hydroxamate inhibitors have potencies in the 10⁻⁹ M range. The only known examples of MMP inhibitors currently being evaluated in clinical trials are hydroxamates such as BB-94 for tumor metastases¹⁷ and Galardin for corneal ulceration.¹⁸ Second-generation hydroxamates, which are reported to be orally bioavailable, are in preclinical evaluation.¹⁹ The potency of the hydroxamates offers the possibility of forming stable enzyme-inhibitor complexes for X-ray crystallographic studies. We, as well as others, have determined the crystal structures of the catalytic domains of human fibroblast collagenase (HFC) and human neutrophil collagenase (HNC) bound to prototypical hydroxamate inhibitors such as 1.²⁰⁻²³ A homology model for human

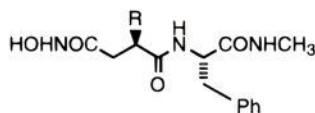
* To whom correspondence and reprint requests should be sent. Present address: 3-Dimensional Pharmaceuticals, Inc., Eagleview Corporate Center, 665 Stockton Dr., Suite 104, Exton, PA 19341.

[†] Department of Medicinal Chemistry.

[‡] Department of Biophysics and Computational Chemistry.

[§] Department of Biochemistry.

[⊙] Abstract published in *Advance ACS Abstracts*, June 1, 1995.

Table 1. Inhibition of MMPs by P₁' Hydroxamate Derivatives

no.	R ^a	K _i (SD), μM		
		HFC	HFS	HNC
1	-CH ₂ CH(CH ₃) ₂	0.007 (0.001)	0.079 (0.007)	0.002 (0.001)
12b	-(CH ₂) ₄ OH	0.064 (0.004)	2.20 (0.48)	0.007 (0.003)
12c	-(CH ₂) ₅ OH	0.031 (0.013)	0.430 (0.22)	0.004 (0.002)
18	-(CH ₂) ₃ COOH ^b	3.35 (0.80)	>10.0	0.270 (0.060)
21a	-(CH ₂) ₃ CONHC ₃ H ₇	5.10 (0.30)	0.360 (0.025)	0.002 (0.001)
21b	-(CH ₂) ₃ CONHCH ₂ Ph	9.6 (.17)	0.092 (0.026)	0.030 (0.005)
21c	-(CH ₂) ₃ CONH(CH ₂) ₂ Ph	1.3 (0.05)	0.006 (0.002)	0.032 (0.002)
29	-(CH ₂) ₄ NHCO(CH ₂) ₂ CH ₃	1.60 (0.23)	0.70 (0.10)	0.012 (0.003)
10a	-(CH ₂) ₃ OCH ₂ Ph	2.27 (0.33)	0.043 (0.008)	<0.001
10b	-(CH ₂) ₄ OCH ₂ Ph	1.45 (0.54)	0.015 (0.004)	0.002 (0.001)
10c	-(CH ₂) ₅ OCH ₂ Ph	0.92 (0.27)	0.019 (0.003)	0.002 (0.001)
14b	-(CH ₂) ₄ OPh	0.008 (0.001)	0.028 (0.002)	<0.002
14c	-(CH ₂) ₅ OPh	0.026 (0.001)	0.014 (0.001)	<0.002

^a Satisfactory elemental analyses were obtained ($\pm 0.4\%$ of calculated values), except where noted. ^b Satisfactory high-resolution mass spectral data and homogeneous by TLC.

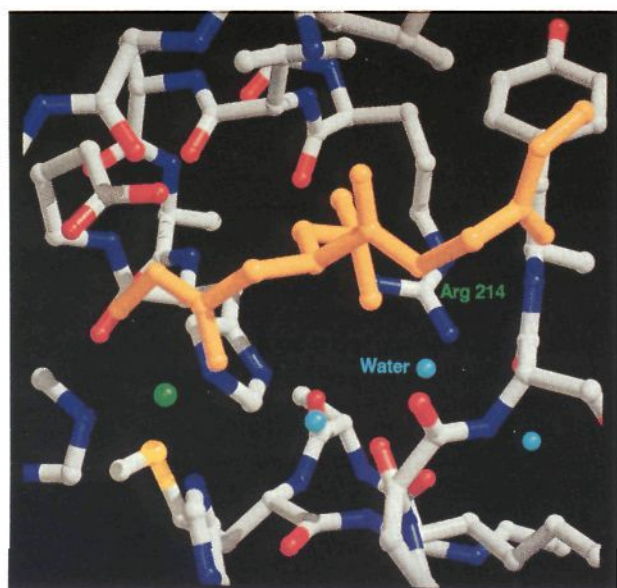


Figure 1. X-ray structure of HFC with bound inhibitor (**1**, yellow) depicting the guanidinium moiety of Arg 214 and the crystallographically observed water molecules (blue spheres). The zinc atom is a green sphere.

fibroblast stromelysin (HFS) was constructed from the HFC and HNC structures and had essentially identical secondary structure.²⁴ The comparative features were utilized as general guidance in the structure-based drug design of novel P₁'-substituted hydroxamate inhibitors. This paper reports in detail and expands the structure-activity relationships (SAR) of a series of hydroxamate inhibitors containing novel P₁' heteroatom-based modifications.²⁵

Rationale

The S₁' pocket of HFC is lined at the bottom by the guanidinium functionality of Arg 214. A structural water molecule is observed in HFC, which forms hydrogen bonds both to the N-H of the guanidinium group and to two backbone carbonyls (Figure 1). In the HNC structure and HFS model, this Arg 214 is replaced by

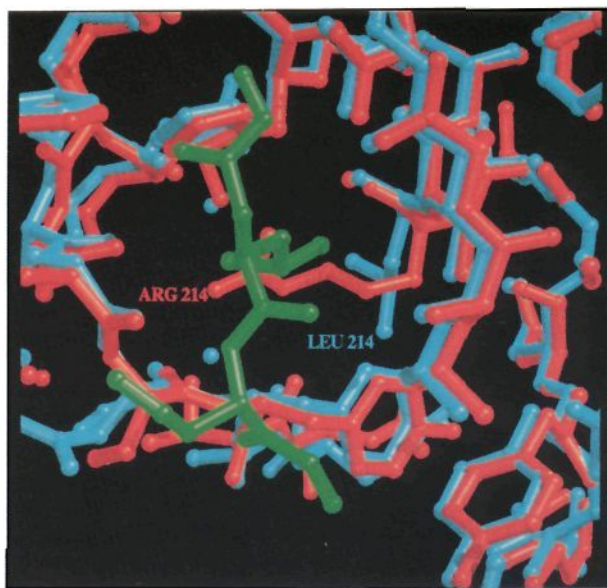


Figure 2. Overlap of the X-ray structures of HFC (red) and HNC (blue) with bound inhibitor (**1**, green) indicating the Arg 214 of HFC versus the Leu 214 of HNC.

Leu 214. This is clearly depicted in Figure 2, which shows an overlap of the HFC (red) and HNC (blue) X-ray structures looking down the S₁' pocket. The guanidinium functionality of Arg 214 in HFC is occupying and blocking the tunnel, which is formed by Leu 214 in HNC. The strategy for HFC inhibitor design was to add functionality to the P₁' group which could (1) form a salt bridge to the guanidinium group of Arg 214 or (2) displace the water molecule to bulk solvent by replacing the hydrogen bonding of the water molecule. The butyric acid **18** appeared to possess the appropriate linker to provide salt bridge formation. The alcohols **12b,c** appeared to possess the appropriate linker to displace the S₁' water molecule and replace its hydrogen-bonding pattern. Also, displacement of the water molecule from the bound site to bulk water should be entropically favorable.

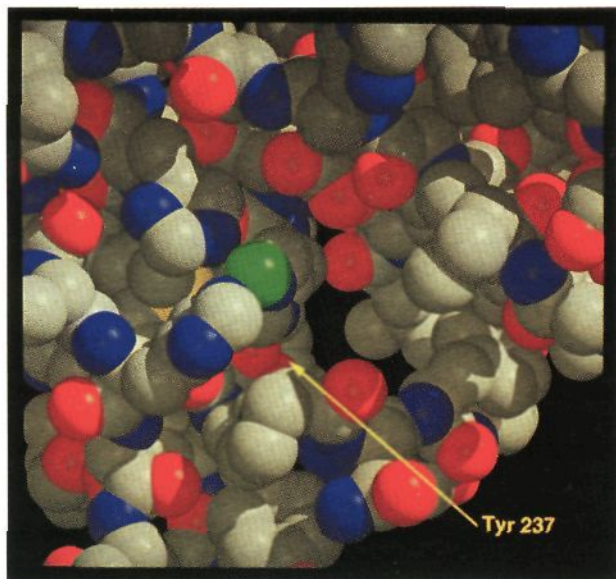


Figure 3. Space-filling depiction of the S_1' pocket of HNC showing the tunnel out to solvent (black opening in center) from the zinc atom (green). The carbonyl of Tyr 237 is pointed out.

In the HNC structure and HFS model, the sterically smaller isobutyl group of Leu 214 does not block off the S_1' pocket, such that a large tunnel out to solvent on the opposite side of the protein is created as depicted by the black hole in the space-filling model of Figure 3. This large tunnel possesses several accessible backbone carbonyls which can form additional hydrogen bonds. In addition, the tunnel can accommodate much larger P_1' substituents which could optimize packing interactions. The butyramides **21a–c** and the acylamine **29** were designed to form a hydrogen bond between the amide N-H of the inhibitors and the carbonyl of Tyr 237 in the larger S_1' pocket of HNC and HFS (Figure 3). All of the above proposed molecules contain protic moieties which would almost certainly be hydrated in the bulk aqueous phase. These molecules would presumably require desolvation in order to occupy the hydrophobic S_1' pocket. If not replaced by specific hydrogen bonding within the S_1' pocket, the desolvation energy cost could result in an increase in observed inhibitory constant (K_i). In order to avoid this desolvation problem, less polar moieties such as the benzylic (**10a–c**) and phenolic (**14b,c**) ethers were proposed for HNC. These large P_1' derivatives would ostensibly occupy the large S_1' pocket of HNC/HFS but not HFC.

Chemistry

The derivatives with three- to five-carbon atom linkers were prepared from intermediates **7** and **9**, the syntheses of which are outlined in Scheme 1. The commercially available diols **2** were O-alkylated with benzyl bromide to give a mixture of mono- (**3**) and dibenzylated products as an approximate 2:1 mixture, which were subsequently used without purification. Each mixture was oxidized using pyridinium dichromate to afford the carboxylates **4** and converted to the acyl chlorides **5** which were subsequently used in the acylation of the chiral auxiliary (*S*)-(-)-4-benzyl-2-oxazolidinone. The anion of **6** was alkylated with *tert*-butyl bromoacetate to give the succinic ester **7**. The

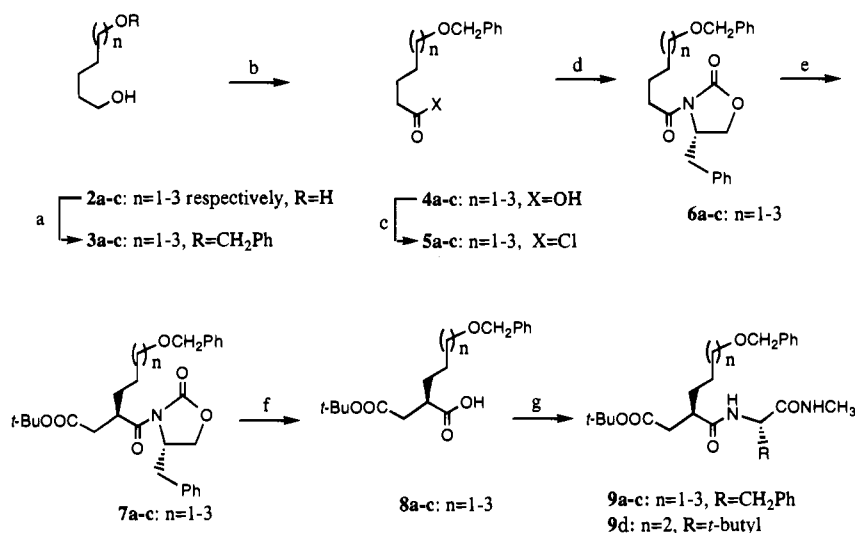
chiral auxiliary was removed by lithium hydroperoxide hydrolysis to produce the chiral succinic acid derivatives **8**. A coupling of **8** with *L*-phenylalanine *N*-methylamide using diethyl cyanophosphonate afforded **9**. The benzylic ether moiety of **7** and **9** was modified to give alcohols and ethers (Scheme 2), acids and amides (Scheme 3), and acylamines (Scheme 4).

The syntheses of the alcohols, benzylic ethers, and phenolic ethers are outlined in Scheme 2. The most straightforward targets which retain the benzylic ether functionality (**10a–c**) were prepared by ester deprotection and formation of the hydroxamate by reaction of the mixed anhydride with *O*-(trimethylsilyl)hydroxylamine (TMSONH₂). The alcohol targets **12b,c** required *O*-debenzylation which could be effected under transfer hydrogenolysis conditions with 20% palladium hydroxide on carbon and 1,4-cyclohexadiene. The resultant alcohols **11b,c** were converted to the hydroxamates **12b,c** in a similar manner as above. The ester deprotection with trifluoroacetic acid (TFA) produced the TFA esters of the hydroxyl group, which subsequently reconverted to the hydroxyl during the workup or purification of the hydroxamates **12b,c**. The phenolic ethers **14b–p** were formed from the alcohol intermediates **11b–d** via Mitsunobu reactions with the requisite substituted phenols.

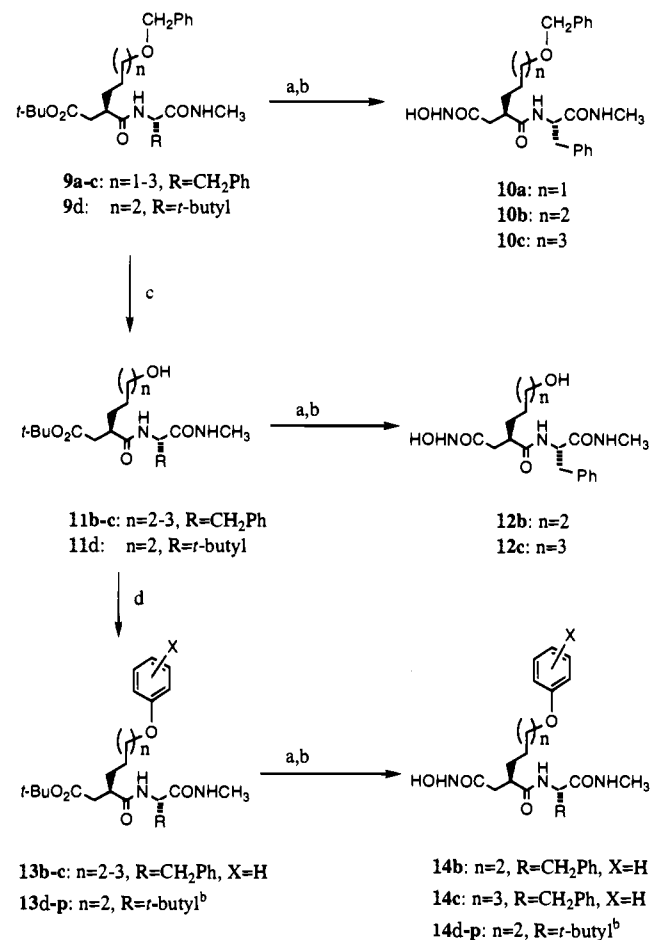
The acid and amide targets were prepared from the butanol intermediate **11b** as outlined in Scheme 3. The carboxylate target **18** was prepared by ester deprotection (**15**) and conversion to the protected *O*-benzyl hydroxamate **16**. The hydroxyl moiety was oxidized to the carboxylate moiety (**17**) using pyridinium dichromate. The deprotection of the hydroxamate with 10% palladium on carbon and a small amount of pyridine yielded **18**. In a different chronology, the butyramides were prepared by initial oxidation and amidation (**20a–c**) followed by elaboration to the hydroxamate by ester deprotection and TMS hydroxylamine reaction.

In order to prepare the acylamine target, the succinic acid intermediate with the chiral auxiliary protection (**7b**) was utilized (Scheme 4). The benzylic ether moiety of **7b** was removed by transfer hydrogenolysis. The resulting alcohol **22** was converted to the mesylate **23** and displaced with sodium azide under phase transfer conditions to give **24**. The azido group was carried through the lithium hydroperoxide hydrolysis and the coupling with *L*-phenylalanine *N*-methylamide (**26**). The azido group was reduced with 5% palladium on carbon and immediately acylated with butyryl chloride to give **27**. The ester deprotection and conversion to hydroxamate produced **29**.

The alcohol intermediate **22** containing the chiral auxiliary for protection was also utilized to prepare the C-terminally modified targets **34a–g** (Scheme 5). In this particular scenario, **22** was reacted under Mitsunobu conditions with *p*-chlorophenol to give **30**. The carboxylate **31**, from lithium hydroperoxide hydrolysis, was coupled with various amides of *tert*-butylglycine (**32a–g**),²⁶ which were synthesized from commercially available Boc-*L*-*tert*-butylglycine. The *tert*-butyl esters **33a–e** were deprotected and converted to the hydroxamates **34a–e** in the usual manner. The *tert*-butyl esters of **33f,g** were deprotected and converted to the corresponding *O*-benzyl hydroxamates. Final hydro-

Scheme 1^a

^a Reagents and conditions: (a) NaH, PhCH₂Br, reflux, THF; (b) pyridinium dichromate, DMF, 10–25 °C; (c) oxalyl chloride; (d) (*S*)-(-)-4-benzyl-2-oxazolidinone, THF, *n*-BuLi, -78 °C; (e) LDA, -78 °C, BrCH₂CO₂*t*-Bu; (f) H₂O₂, LiOH; (g) diethyl cyanophosphonate, DMF, 0 °C, *L*-phenylalanine *N*-methylamide (R = CH₂Ph) or *L*-*tert*-butylglycine *N*-methylamide (R = *tert*-Bu).

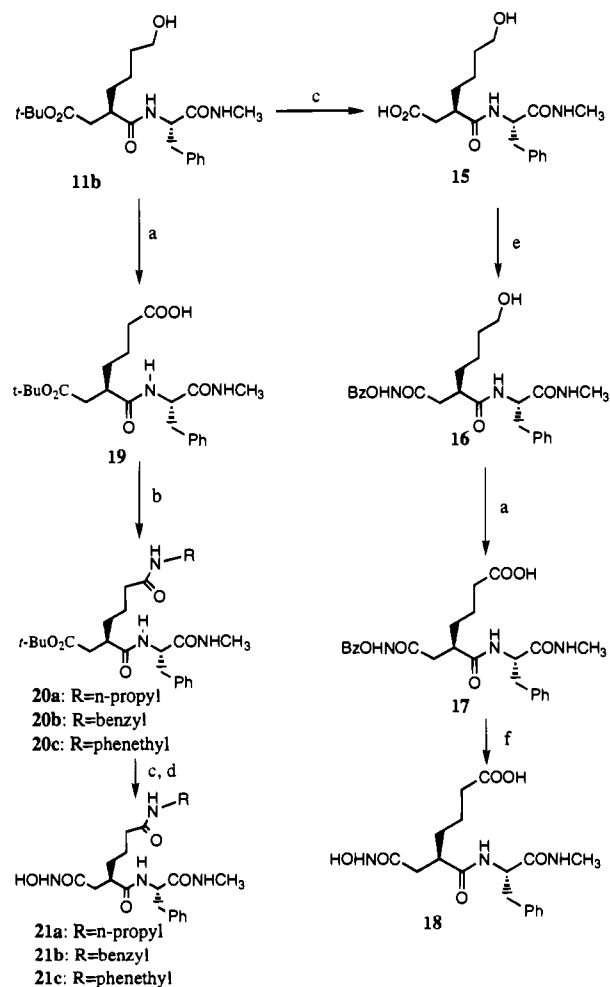
Scheme 2^a

^a Reagents and conditions: (a) TFA, rt; (b) isobutyl chloroformate, NMM, TMSONH₂; (c) 20% Pd(OH)₂/C, 1,4-cyclohexadiene; (d) PPh₃, DEAD, phenols.^b X as described in Table 2.

genolysis of both the *O*-benzyl hydroxamate and benzyl ester moieties afforded **34f,g**.

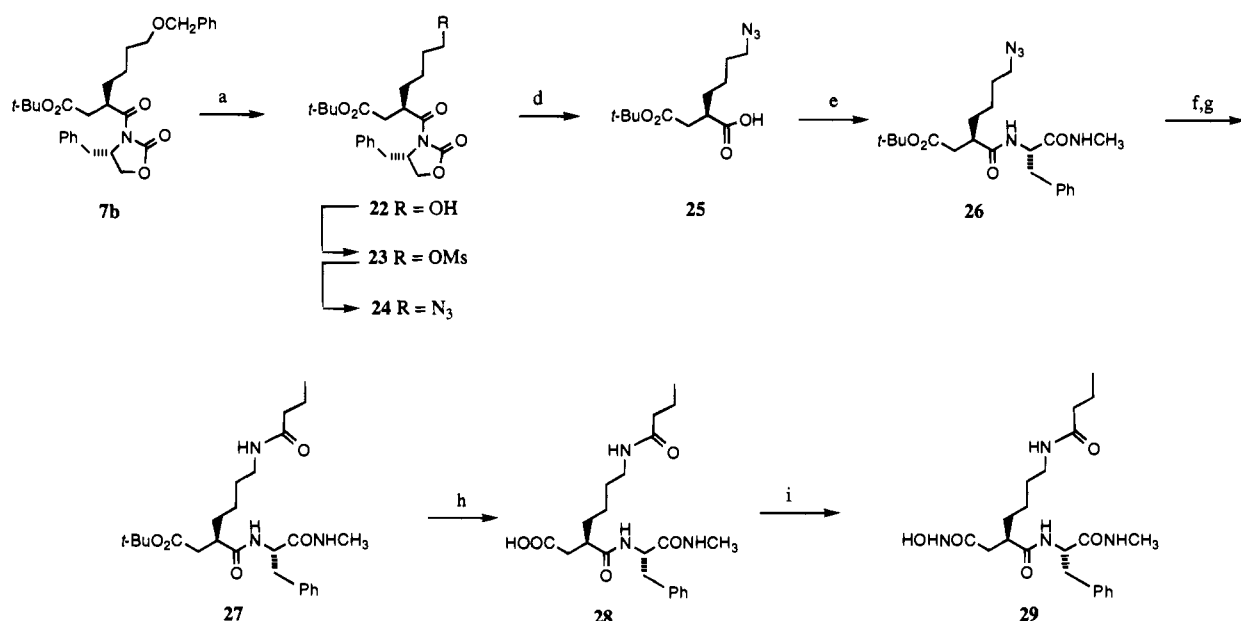
Results and Discussion

The inhibitory potencies of the aforementioned inhibitors were determined against the stable truncated

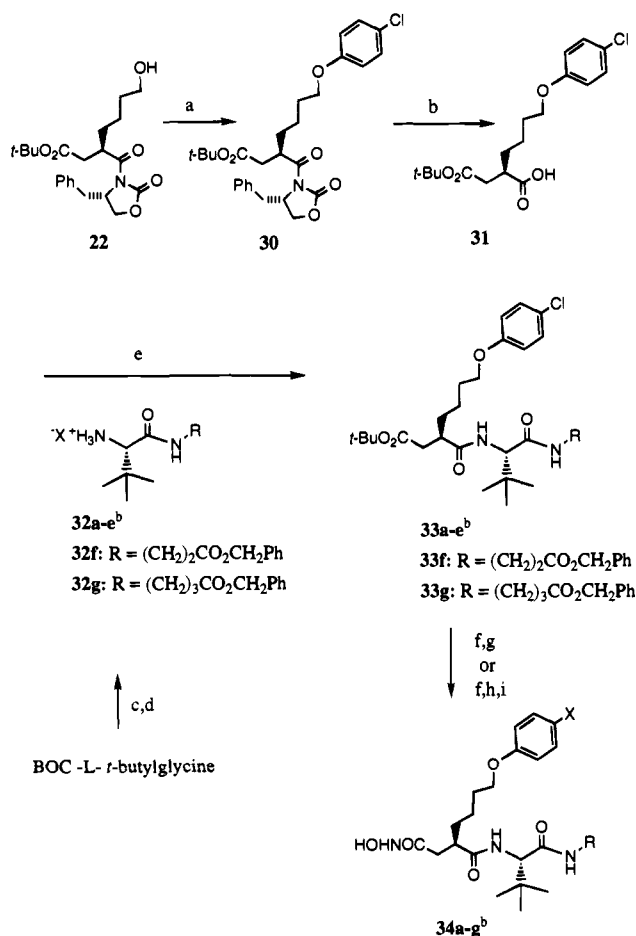
Scheme 3^a

^a Reagents and conditions: (a) PDC, DMF; (b) RNH₂, DEPC, Et₃N (R = *n*-propyl, benzyl, phenethyl); (c) TFA; (d) isobutyl chloroformate, NMM, TMSONH₂; (e) isobutyl chloroformate, NMM, BzONH₂; (f) 10% Pd/C, H₂, pyridine, ethanol.

versions of HFC, HFS, and HNC.²⁷ The targeting of HFC involved the displacement of a crystallographically observed water molecule or the complementary binding

Scheme 4^a

^a Reagents and conditions: (a) 20% Pd(OH)₂, 1,4-cyclohexadiene, (b) MsCl; (c) NaN₃; (d) LiOH, H₂O₂; (e) L-phenylalanine *N*-methylamide, DEPC, Et₃N; (f) 5% Pd/C, H₂; (g) C₃H₇COCl, NEt₃; (h) TFA; (i) NMM, isobutyl chloroformate, TMSONH₂.

Scheme 5^a

^a Reagents and conditions: (a) 4-chlorophenol, Ph₃P, DEAD; (b) LiOH, H₂O₂; (c) DEPC, NEt₃ or isobutyl chloroformate, NMM, RNH₂; (d) TFA or HCl; (e) DEPC, NEt₃; (f) TFA; (g) isobutyl chloroformate, NMM, TMSONH₂; (h) isobutyl chloroformate, NMM, BzONH₂; (i) 5% Pd/C, H₂, pyridine.^b R and X as described in Table 3.

to the guanidinium moiety of Arg 214. The butyric acid **18**, which was designed to provide a salt bridge to the

basic guanidinium moiety of Arg 214, was several orders of magnitude less potent across the MMP panel than the prototypical hydroxamate inhibitor **1**. The energy gain of a specific salt-bridge interaction was estimated to be larger than the energy cost of desolvation.²⁸ Thus, the net result should be an increase in potency. The data of **18**, which was uniformly less potent against all MMPs, would argue that salt-bridge formation was not accomplished. The alcohols **12b,c**, which were designed to replace the observed water molecule in HFC, were not more potent than the P₁' isobutyl (**1**). The rationale to displace the crystallographically observed water molecule should lead to an entropic gain in binding energy.²⁹ This water molecule donates two hydrogen bonds and accepts one hydrogen bond in the HFC crystal structure. The alcohols **12b,c** could replace two of these hydrogen bond interactions. The net effect from an entropic gain in binding energy due to displacement of the water molecule and the energy cost due to loss of a hydrogen bond interaction is undetermined. The hypothesis is further complicated by the energy cost associated with the desolvation of the hydroxyl moiety of the inhibitor. Whether the water molecule was indeed displaced awaits crystallographic confirmation, but the strategy was unsuccessful in increasing potency.

The targeting of HNC and HFS involved the formation of specific hydrogen bonds to the accessible backbone carbonyls in the large S₁' pocket. These inhibitors would not be expected to be potent HFC inhibitors because the size of the S₁' pocket is delimited by the side chain of Arg 214. The results for the butyramides **21a-c** and acylamine **29** are consistent with this hypothesis: all show micromolar potencies against HFC (1.3–9.6 μM) while showing submicromolar potencies against HFS and HNC.

Although the HFS homology model was essentially identical to the X-ray structure of HNC, it was surprising to observe inhibitors with switched selectivity. For example, within the butyramide series, **21a** was selective for HNC while **21c** was slightly selective for HFS.

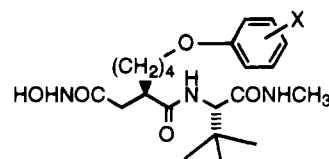
The *N*-propylbutyramide **21a** was the most selective HNC inhibitor by 2 and 3 orders of magnitude in potency versus HFS and HFC, respectively. However, the *N*-phenethylbutyramide **21c** was more potent against HFS than HNC and represents a 60-fold increase in HFS potency over **21a**. These potencies may indicate a successful hydrogen bond formation in the S_1' pocket of HNC with **21a** and of HFS with **21c**, especially in light of the potential desolvation energy cost associated with the amide functionality. The proof that **21a,c** have located a specific hydrogen bond to Tyr 237 in the S_1' pocket of HNC and HFS, respectively, awaits enzyme-inhibitor crystallographic evidence.

The second strategy to target HFS and HNC involved the optimization of space-filling the S_1' pocket without the inherent desolvation energy problem associated with polar moieties. Thus, large P_1' derivatives containing benzylic (**10a–c**) and phenolic (**14b,c**) ether moieties were designed. The results of the benzylic ethers (**10a–c**) show the expected micromolar potencies against HFC and the nanomolar potencies against HFS and HNC. However, surprising results for HFC were obtained when the ether oxygen was transposed from the benzylic position to the phenolic position. A comparison of ethers of similar overall length (**10a** vs **14b**, **10b** vs **14c**) indicated a unique potency against HFC for phenolic ethers (**14b,c**), which would appear to be too large to occupy the S_1' pocket of HFC. Molecular mechanics minimization of these enzyme-inhibitor complexes in which the protein side chains were relaxed suggested that the side chain of Arg 214 might be displaced such that a π - π interaction³⁰ is formed between the electron-rich phenolic moiety³¹ and the electron-poor guanidinium moiety. Another possibility is a completely different mode of binding than that observed for **1**. The proof relies on further crystallographic studies of the enzymes with these inhibitors.

The unique potent and nonselective profile of the phenolic inhibitors **14b,c** provided a focus for further structure-activity studies (Table 2). The SAR of the phenolic ring was studied against HFC and HFS for hydroxamates containing *tert*-butylglycine *N*-methylamide at P_2' . As judged by docking studies to the HNC structure/HFS model,³² para-substitution appeared to provide the optimal occupation of the large S_1' tunnel. This hypothesis was verified by the potent (6–41 nM) inhibition of HFS by virtually all of the para-substituents (**14d–l**), even the sterically large *n*-pentyl derivative **14i**. The meta-substituents **14m–p** were slightly less potent (62–112 nM) against HFS. On the other hand, the potency against HFC was more sensitive. The elongation of the para-substituent from H (**14d**) to *n*-pentyl (**14i**) caused a potency decrease of approximately 3 orders of magnitude (3 nM to 1.9 μ M). The *p*-chlorophenol **14j** was judged to be protective against metabolism in the para-position of the phenol ring. Preliminary *in vitro* tissue slice metabolism studies supported this hypothesis.³³

The SAR of the C-terminal amide was studied for hydroxamates containing P_1' (*p*-chlorophenoxy)butyl and P_2' *L*-*tert*-butylglycine (Table 3). The variations of C-terminal amides ranged from two- to three-carbon linkers with either weakly basic (**34a,b,e**), neutral polar (**34c**), neutral lipophilic (**34d**), and acidic (**34f,g**) moieties at the terminus. Compared to the *N*-methylamide

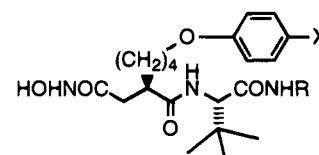
Table 2. Inhibition of MMPs by Substituted Phenolic Ether Analogs



no.	X	formula ^a	K_i (SD), μ M	
			HFC	HFS
14d	H	$C_{21}H_{33}N_3O_5 \cdot 0.50H_2O$	0.003 (0.001)	0.006 (0.004)
14e	4-CH ₃	$C_{22}H_{35}N_3O_5$	0.014 (0.003)	0.017 (0.001)
14f	4-C ₃ H ₇	$C_{24}H_{39}N_3O_5 \cdot 0.50H_2O$	0.17 (0.03)	0.011 (0.005)
14g	4- <i>i</i> -C ₃ H ₇	$C_{24}H_{39}N_3O_5 \cdot 0.50H_2O$	0.30 (0.09)	0.012 (0.005)
14h	4- <i>t</i> -C ₄ H ₉	$C_{25}H_{41}N_3O_5 \cdot 0.50H_2O$	0.35 (0.08)	0.016 (0.009)
14i	4-C ₅ H ₁₁	$C_{26}H_{43}N_3O_5 \cdot 0.50H_2O$	1.9 (0.50)	0.014 (0.007)
14j	4-Cl	$C_{21}H_{32}N_3O_5Cl \cdot 0.25H_2O$	0.021 (0.001)	0.009 (0.0004)
14k	4-F	$C_{21}H_{33}N_3O_5F$	0.011 (0.001)	0.038 (0.008)
14l	4-OCH ₃	$C_{22}H_{35}N_3O_6$	<0.001	0.041 (0.024)
14m	3-CH ₃	$C_{22}H_{35}N_3O_5$	0.016 (0.005)	0.054 (0.023)
14n	3-Cl	$C_{21}H_{33}N_3O_5 \cdot 0.25H_2O$	0.143 (0.017)	0.112 (0.022)
14o	3-OCH ₃	$C_{22}H_{35}N_3O_6$	0.072 (0.014)	0.065 (0.011)
14p	3,4-Cl ₂	$C_{21}H_{31}N_3O_5Cl_2 \cdot 0.25H_2O$	0.095 (0.020)	0.062 (0.019)

^a Satisfactory elemental analyses were obtained ($\pm 0.4\%$ of calculated values).

Table 3. Inhibition of MMPs by C-Terminal Modifications of Phenolic Ethers



no.	R ^a	X	K_i (SD), μ M	
			HFC	HFS
34a	-(CH ₂) ₂ -1-pyrrolidino ^b	Cl	0.08 (0.01)	0.005 (0.001)
34b	-(CH ₂) ₃ -1-morpholino ^b	Cl	0.010 (0.008)	<0.002
34c	-(CH ₂) ₂ -Ph- <i>p</i> -SO ₂ NH ₂	Cl	0.061 (0.018)	<0.002
34d	-(CH ₂) ₂ -Ph	Cl	0.58 (0.30)	0.005 (0.001)
34e	-(CH ₂) ₂ -2-pyridyl ^b	Cl	0.08 (0.01)	0.006 (0.002)
34f	-(CH ₂) ₂ -COOH ^b	H	0.14 (0.02)	0.003 (0.001)
34g	-(CH ₂) ₃ -COOH ^b	H	0.062 (0.027)	0.002 (0.0005)

^a Satisfactory elemental analyses were obtained ($\pm 0.4\%$ of calculated values), except where noted. ^b High-resolution mass spectral and NMR data.

14j, all of these variations, except the phenethyl amide **34d**, retained potent inhibition against HFC and HFS (within 1 order of magnitude). Within this limited data set, the inhibitors with longer three-carbon linkers (**34b,g**) were more potent than those with two-carbon linkers (**34a,c–f**).

Conclusions

The structure-based drug design strategies which appear to have been successful as judged by the inhibitory potencies were specific hydrogen bonding in the S_1' pocket, space filling of the large S_1' pocket, and a π - π interaction between guanidinium and phenolic groups.

The HNC specific inhibitors **21a** and **29** were hypothesized to form a specific hydrogen bond to a backbone carbonyl of Tyr 237, although these have not been verified. The potent HFS/HNC inhibitor **21c** may form a similar hydrogen bond in both enzymes. The benzylic ethers **10a–c** provide good space filling of the large S_1' tunnel of the HFS and HNC. In general, the potent, nonselective MMP inhibitors contain electron-rich phenolic ether moieties, which have the potential to form a π - π interaction with the electron-deficient guanidinium moiety of Arg 214 of HFC. It is hoped that the availability of these potent, selective and nonselective inhibitors will aid in the elucidation of the role of MMPs in both normal and disease states.

Experimental Section

Biology. The cDNA for human fibroblast collagenase and stromelysin was obtained from G. I. Goldberg.³⁴ The cDNA for human neutrophil collagenase was obtained from N. Berliner.³⁵ The expression vector construction, expression, purification of inclusion bodies, and folding of inclusion bodies were performed as described.³⁶ Fibroblast collagenase was expressed as a proenzyme with a C-terminal truncation, Phe 1-Pro 250. HFC was activated by incubation with 1 mM (*p*-aminophenyl)mercury, and the catalytic domain was purified from the propeptide fragments by gel filtration. This resulted in a mixture of N-termini starting with Val 82 and Leu 83. Fibroblast stromelysin and neutrophil collagenase were expressed as mature enzymes with C-terminal truncations Phe 83-Thr 260 and Met 81-Gly 243, respectively. The concentration of catalytic domain was determined from the A_{280} and the extinction coefficient calculated from the Tyr and Trp content deduced from the cDNA sequence.³⁷ These values are 25.5, 28.5, and 27.0 $\text{mM}^{-1} \text{cm}^{-1}$ for the catalytic domains of HFC, HNC, and HFS, respectively. Due to autolysis, these values overestimate the concentration of active HNC slightly and active HFS significantly.

A typical assay contained, in a microtiter plate well, 4 nM MMP in 100 μL of 0.05 M tricine, pH 7.5, 0.2 M NaCl, 10 mM CaCl_2 , 0.05% Brij-35, 0.02% sodium azide (buffer), and 300 μM benzoyl-Pro-Leu-Ala-Leu-Tyr(OMe)-N(CH₂)₄NMe₂. After 30 min incubation at 37 °C, the enzymatic reaction was stopped by the addition of 25 μL of 1 mM 1,10-phenanthroline in buffer/10% dioxane. The product, H-Leu-Tyr(OMe)-N-butyl-NMe₂, was determined fluorometrically (Titertek fluorskan II) after a 30 min reaction at 22 °C with 25 μL of 5.5 mg/mL fluoescamine in dioxane. Inhibitors were dissolved in DMSO, and their concentration was determined optically after $1/20$ dilution in 2% ferric chloride in 0.1 N HCl, using the extinction coefficient $E_{540} = 0.9 \text{ mM}^{-1}$.³⁸ Inhibitors were diluted by serial 2-fold dilutions, with the maximum final DMSO concentration <3%. IC₅₀ values were converted to K_i values using $K_i = \text{IC}_{50}/(1 + S/K_m)$. The K_m values (μM) used for the above deviations were calculated from the K_i values of three or more separate experiments.

Chemistry. General Procedures. All solvents were HPLC grade and used as received with the exception of THF which was either SureSeal (Aldrich Chemical Co., Milwaukee, WI) or freshly distilled from sodium benzophenone ketyl. Proton NMR spectra were recorded on a Varian Gemini-300 NMR spectrometer. Low- and high-resolution mass spectra (HRMS) were determined using liquid secondary ion mass spectrometry (LSIMS) on a Kratos Concept spectrometer. Analytical results for compounds followed by elemental symbols are $\pm 0.4\%$ of calculated values unless otherwise indicated and were determined by Quantitative Technologies, Inc., Whitehouse, NJ. Melting points were recorded on a Thomas Hoover capillary melting point apparatus and are uncorrected. Preparative flash column chromatography was performed on silica gel 60 (E. Merck; 230–400 mesh).

6-(Phenylmethoxy)hexan-1-ol (3b). Hexane-1,6-diol, **2b** (25 g, 0.21 mol), was dissolved in dry/distilled THF (300 mL) under a nitrogen atmosphere and treated with 80% NaH (6.3

g, 0.21 mol) in small portions over 10–20 min with vigorous stirring. The reaction mixture was heated to reflux with continued vigorous stirring for 4.5 h. Next, benzyl bromide (25 mL, 0.21 mol) was added in one portion and the reaction mixture heated at reflux for 22 h. After cooling to room temperature, the reaction mixture was filtered, and the solid (NaBr) was washed with THF. The combined THF filtrates were evaporated to a yellow oil. The oil was taken up in Et₂O and washed repeatedly with H₂O until there was no indication of the starting diol (as followed by TLC) and then with brine. The organic layer was dried over Na₂SO₄ and filtered and the Et₂O evaporated. The resulting oil (38.05 g, 50–60%) was a mixture of the mono- and dibenzylated product (approximately a 2:1 ratio of mono:di based on ¹H-NMR) and was used without further purification in the next step. A small amount of **3b** was isolated via silica gel column chromatography (0–25% EtOAc/hexane). ¹H-NMR (CDCl₃): δ 1.3–1.7 (m, 9H), 3.5 (t, 2H), 3.64 (t, 2H), 4.5 (s, 2H), 7.3 (m, 5H).

3a,c were synthesized in an analogous procedure and isolated as oils in 50–60% yield.

6-(Phenylmethoxy)hexanoic Acid (4b). A solution of **3b** (38 g, 0.114 mol) in dry DMF (150 mL) was added dropwise to a solution of pyridinium dichromate (PDC) (128 g, 0.342 mol) in DMF (300 mL). The reaction was slightly exothermic, and thus the mixture was maintained at 10 °C for 2 h with a cool water bath. The reaction mixture was stirred for 9 h at room temperature, diluted with 2.5 L of H₂O, and extracted repeatedly with Et₂O. The combined extracts were washed with H₂O; filtering the organic solution through Celite helped remove any remaining PDC. The organic layer was then extracted with 0.5 N NaOH (5 \times 100 mL), and the combined basic extractions were washed with several portions of fresh Et₂O. The basic layer was then cooled, slowly acidified with concentrated HCl to a pH 2–3, and then extracted with Et₂O. The combined organic layers were dried over Na₂SO₄ and then filtered. Evaporation of the solvent afforded pure **4b** (19.0 g, 75%) as a yellow oil. ¹H-NMR (CDCl₃): δ 1.45 (m, 2H), 1.65 (m, 4H), 2.35 (t, 2H), 3.47 (t, 2H), 4.5 (s, 2H), 7.3 (m, 5H). HRMS: m/z found, 223.13245 (MH⁺); C₁₃H₁₉O₃ requires 223.13342.

4a,c were synthesized in an analogous procedure and isolated as oils. **4a**: 66% yield. HRMS: m/z found, 209.11777 (MH⁺); C₁₂H₁₇O₃ requires 209.11777. **4c**: 60% yield. HRMS: m/z found, 235.13242 (M – H⁺); C₁₄H₁₉O₃ requires 235.13342. Anal. (C₁₄H₂₀O₃) C, H.

6-(Phenylmethoxy)hexanoyl Chloride (5b). Compound **4b** (30.52 g, 0.14 mol) was dissolved in dry CH₂Cl₂ (200 mL) and cooled to 0 °C under a nitrogen atmosphere. Oxalyl chloride (13.09 mL, 0.154 mol) was then added in one portion. Some gas evolution (CO₂) was observed. After 5 drops of dry DMF was added with stirring, the gas evolution became more vigorous. The reaction mixture was stirred while warming slowly to room temperature until no additional gas evolution was observed, and then for 30 min more. The CH₂Cl₂ and remaining oxalyl chloride were removed under vacuum, leaving a yellow oil with some solid dispersed in it. The oil was filtered through a dry filter into a dry flask, giving **5b** (29.6 g, 90%) as a yellow oil. ¹H-NMR (CDCl₃): δ 1.45 (m, 2H), 1.6–1.82 (m, 4H), 2.9 (t, 2H), 3.48 (t, 2H), 4.5 (s, 2H), 7.35 (m, 5H).

5a,c were synthesized in an analogous procedure and isolated as yellow oils in 85–94% yield.

(4S)-4-Benzyl-3-[(6'-phenylmethoxy)hexanoyl]-2-oxazolidone (6b). (S)-(-)-4-Benzyl-2-oxazolidinone (21.08 g, 0.12 mol) was dissolved in dry/distilled THF (250 mL) and cooled to –78 °C under a nitrogen atmosphere; 1.6 M *n*-BuLi in hexane (74.77 mL, 0.12 mol) was added dropwise with stirring while maintaining the temperature between –65 and –78 °C. The reaction mixture was stirred at –78 °C for 25 min, and then **5b** (28.8 g, 0.12 mol) in THF (100 mL) was added dropwise, again maintaining the temperature near –78 °C. The reaction mixture was allowed to gradually warm to room temperature and then the reaction quenched with the addition of a saturated solution of NH₄Cl (150 mL). The THF was evaporated and the residue extracted with Et₂O. The combined extracts were washed with 0.5 N NaOH, H₂O, and brine and then dried over Na₂SO₄ and filtered. The solvent

was evaporated, and the oil residue was purified by flash chromatography on silica gel (15–40% EtOAc/hexane), affording **6b** (46.5 g, 85%) as a pale yellow oil. $^1\text{H-NMR}$ (CDCl_3): δ 1.5 (m, 2H), 1.6–1.8 (m, 4H), 2.77 (dd, 1H), 2.95 (m, 2H), 3.3 (dd, 1H), 3.5 (t, 2H), 4.17 (m, 2H), 4.5 (s, 2H), 4.67 (m, 1H), 7.3 (m, 10H). HRMS: m/z found, 382.20138 (MH^+); $\text{C}_{29}\text{H}_{28}\text{NO}_4$ requires 382.20183.

6a,c were synthesized in an analogous procedure and isolated as pale yellow oils. **6a**: 64% yield. HRMS: m/z found, 368.18543 (MH^+); $\text{C}_{22}\text{H}_{26}\text{NO}_4$ requires 368.18618. **6c**: 53% yield. HRMS: m/z found, 394.20349 ($\text{M} - \text{H}^+$); $\text{C}_{24}\text{H}_{26}\text{NO}_4$ requires 394.20183.

(4S)-4-Benzyl-3-[(2R)-2'-[(tert-butoxycarbonyl)methyl]-6'-(phenylmethoxy)hexanoyl]-2-oxazolidone (7b). Diisopropylamine (1.82 mL, 13 mmol) in dry/distilled THF (10 mL) was cooled to -10°C under a nitrogen atmosphere; 1.6 M *n*-BuLi in hexane (8.12 mL, 13 mmol) was slowly added dropwise with stirring while maintaining the temperature below 0°C . The reaction mixture was stirred at 0°C for 30 min and then cooled to -78°C . Compound **6b** (4.71 g, 12 mmol) in THF (50 mL) was then added dropwise with stirring while maintaining the temperature near -78°C . Stirring was continued for 30 min, and then *tert*-butyl bromoacetate (1.8 mL, 12 mmol) in THF (25 mL) was added dropwise at -78°C . The reaction mixture was stirred while slowly warming to room temperature and then the reaction quenched cautiously with H_2O . The THF was evaporated and the residue extracted with EtOAc. The organic layer was washed with 5% NaHCO_3 , 5% citric acid, and brine and then dried over Na_2SO_4 and filtered. The solvent was evaporated, and the resulting oil solidified on standing. The solid product was recrystallized with EtOAc/hexane, affording **7b** (3.21 g, 55%) as white crystals: mp $100\text{--}101^\circ\text{C}$. $^1\text{H-NMR}$ (CDCl_3): δ 1.4–1.72 (m, 15H), 2.48 (dd, 1H), 2.75 (2 overlapping dd, 2H), 3.34 (dd, 1H), 3.45 (t, 2H), 4.15 (m, 3H), 4.48 (s, 2H), 4.63 (m, 1H), 7.3 (m, 10H). Anal. ($\text{C}_{29}\text{H}_{37}\text{NO}_6$) C, H, N.

7a,c were synthesized in an analogous procedure. **7a** was isolated as a pale yellow oil via silica gel column chromatography (5–30% EtOAc/hexane) in 50% yield. HRMS: m/z found, 480.23851 ($\text{M} - \text{H}^+$); $\text{C}_{28}\text{H}_{34}\text{NO}_6$ requires 480.23861. **7c** was isolated as white crystals, recrystallized from EtOAc/hexane in 57% yield: mp $67\text{--}68^\circ\text{C}$. Anal. ($\text{C}_{30}\text{H}_{39}\text{NO}_6$) C, H, N.

(2R)-2-[(tert-Butoxycarbonyl)methyl]-6-(phenylmethoxy)hexanoic Acid (8b). Compound **7b** (0.5 g, 1 mmol) was dissolved in a 4:1 THF/ H_2O solution (15 mL) and cooled to $\sim 2^\circ\text{C}$ under a nitrogen atmosphere. The temperature was not allowed to go below 0°C ; 30% aqueous H_2O_2 (0.5 mL, 4.4 mmol) was then added slowly via syringe while maintaining the temperature below 5°C . After stirring 5 min, $\text{LiOH}\cdot\text{H}_2\text{O}$ (0.07 g, 1.5 mmol) in H_2O (2 mL) was added via syringe. Some gas evolution was observed. The reaction mixture was stirred for 10 min and then warmed to room temperature and stirred for 1 h. The reaction mixture was again cooled in an ice bath, and Na_2SO_3 (0.2 g, 1.7 mmol) in H_2O (2 mL) was added dropwise. After stirring for 20 min, the THF was evaporated and the remaining basic layer was extracted with EtOAc. These EtOAc extracts contained free (*S*)-(-)-4-benzyl-2-oxazolidinone which was recrystallized and recycled for further use. The basic layer was cooled and acidified with the slow addition of concentrated HCl to a pH of 2–3. The cloudy mixture was extracted with EtOAc, and the combined extracts were dried over Na_2SO_4 and filtered. Evaporation of the solvent gave the acid **8b** (0.29 g, 86%) as a colorless oil. $^1\text{H-NMR}$ (CDCl_3): δ 1.4–1.73 (m, 15H), 2.37 (dd, 1H), 2.6 (dd, 1H), 2.8 (m, 1H), 3.45 (t, 2H), 4.5 (s, 2H), 7.3 (m, 5H). Anal. ($\text{C}_{19}\text{H}_{28}\text{O}_5\cdot 0.25\text{H}_2\text{O}$) C, H.

8a,c were synthesized in an analogous procedure and isolated as colorless oils. **8a**: 94% yield. **8c**: 88% yield. HRMS: m/z found, 349.20005 ($\text{M} - \text{H}^+$); $\text{C}_{20}\text{H}_{29}\text{O}_5$ requires 349.20150.

N-[(2R)-2-[(tert-Butoxycarbonyl)methyl]-6-(phenylmethoxy)hexanoyl]-L-phenylalanine N-Methylamide (9b). Compound **8b** (3.36 g, 0.01 mol) and L-phenylalanine N-methylamide TFA salt (2.9 g, 0.01 mol) were dissolved in dry DMF (40 mL) and cooled to -10°C under a nitrogen atmo-

sphere. Diethyl cyanophosphonate (1.52 mL, 0.01 mol) followed by Et_3N (4.18 mL, 0.03 mol) was then added dropwise via syringe. The reaction mixture was stirred for 1 h at -10°C and then at room temperature for 2 h. The DMF was evaporated and the residue taken up into EtOAc. The EtOAc layer was then washed with 5% NaHCO_3 , 5% citric acid, H_2O , and brine, dried over Na_2SO_4 , and filtered. The solvent was evaporated and the residue purified via silica gel column chromatography (50–70% EtOAc/hexane), affording **9b** (4.21 g, 85%) as a gum. $^1\text{H-NMR}$ (CDCl_3): δ 1.20–1.80 (m, 15H), 2.25–2.60 (m, 3H), 2.65 (d, 3H), 3.38 (t, 2H), 3.07 (d, 2H), 4.44 (s, 2H), 4.57 (q, 1H), 6.34 (q, 1H), 6.52 (d, 1H), 7.20–7.60 (m, 10H). MS: m/z 497 (MH^+). Anal. ($\text{C}_{29}\text{H}_{40}\text{N}_2\text{O}_5$) C, H, N.

9a,c were synthesized in an analogous procedure and isolated as gums. **9a**: 74% yield. HRMS: m/z found, 483.28650 (MH^+); $\text{C}_{28}\text{H}_{39}\text{N}_2\text{O}_5$ requires 483.28590. **9c**: 74% yield. HRMS: m/z found, 5.11.31713 (MH^+); $\text{C}_{30}\text{H}_{43}\text{N}_2\text{O}_5$ requires 5.11.31720. Anal. ($\text{C}_{30}\text{H}_{42}\text{N}_2\text{O}_5$) C, H, N.

9d was synthesized in an analogous procedure, substituting (2*S*)-2-amino-3,3-dimethylbutanoic acid *N*-methylamide hydrochloride for L-phenylalanine *N*-methylamide TFA salt. The crude product was isolated as a colorless oil and used in the synthesis of **11d** without further purification: 91% yield. $^1\text{H-NMR}$ (CDCl_3): δ 1.00 (s, 9H), 1.2–1.75 (m, 15H), 2.30–2.70 (m, 3H), 2.80 (d, 2H), 3.45 (t, 2H), 4.25 (d, 1H), 4.50 (s, 2H), 6.15 (br s, 1H), 6.55 (d, 1H), 7.2–7.5 (m, 5H). HRMS: m/z found, 463.31537 (MH^+); $\text{C}_{26}\text{H}_{43}\text{N}_2\text{O}_5$ requires 463.31720.

N-[(2R)-2-[2'-(Hydroxyamino)-2'-oxoethyl]-6-(phenylmethoxy)hexanoyl]-L-phenylalanine N-Methylamide (10b). A solution of **9b** (0.33 g, 0.66 mmol) dissolved in TFA (7 mL) and H_2O (3 mL) was stirred at room temperature until the *tert*-butyl ester was consumed (as followed by TLC). The TFA and H_2O were then evaporated, and the residue was triturated in Et_2O , producing a white solid. The solid was filtered, triturated with fresh Et_2O , and dried *in vacuo*, yielding the acid of **9b** (0.227 g, 78%) as a white solid: mp $150\text{--}151^\circ\text{C}$. $^1\text{H-NMR}$ ($\text{MeOH-}d_4$): δ 0.80–1.50 (m, 6H), 2.00–2.60 (m, 6H), 2.74 and 2.92 (2 dd, 2H), 3.20 (t, 2H), 4.25 (m, 3H), 6.90–7.30 (m, 10H). Anal. ($\text{C}_{25}\text{H}_{32}\text{N}_2\text{O}_5$) C, H, N.

Acids of **9a,c** were synthesized in an analogous procedure and isolated as white solids. Acid of **9a**: 57% yield. Mp: $117\text{--}20^\circ\text{C}$. Anal. ($\text{C}_{24}\text{H}_{30}\text{N}_2\text{O}_5$) C, H, N. Acid of **9c**: 72% yield. Mp: $147\text{--}149^\circ\text{C}$. Anal. ($\text{C}_{26}\text{H}_{34}\text{N}_2\text{O}_5$) C, H, N.

The acid of **9b** (0.44 g, 1.0 mmol) was dissolved in dry/distilled THF (5 mL) and cooled to -10°C under a nitrogen atmosphere. *N*-Methylmorpholine (0.13 mL, 1.15 mmol) followed by isobutyl chloroformate (0.15 mL, 1.15 mmol) was then added via syringe with stirring. The solution became slightly cloudy. The reaction mixture was stirred for 20 min at -10°C ; then *O*-(trimethylsilyl)hydroxylamine (0.12 mL, 1.15 mmol) was added via syringe. After stirring for 2 h at -10°C , the reaction mixture was filtered and the solvent evaporated. The residue was triturated in CH_2Cl_2 , producing a white solid. The solid was washed with CH_2Cl_2 and dried *in vacuo*. This afforded the hydroxamate **10b** (0.27 g, 59%) as a white solid: mp $147\text{--}150^\circ\text{C}$. $^1\text{H-NMR}$ ($\text{MeOH-}d_4$): δ 1.6–1.1 (m, 6H), 2.10 (dd, 1H), 2.22 (dd, 1H), 2.60 (m, 1H), 2.64 (d, 3H), 2.96 (dd, 1H), 3.15 (dd, 1H), 3.40 (t, 2H), 4.46 (s, 2H), 4.49 (m, 1H), 7.35–7.10 (m, 10H), 7.90 (m, 1H), 8.20 (d, 1H). Anal. ($\text{C}_{25}\text{H}_{33}\text{N}_3\text{O}_5\cdot 0.25\text{H}_2\text{O}$) C, H, N.

10a,c were synthesized in an analogous procedure and isolated as white solids. **10a**: 79% yield. Mp: $147\text{--}149^\circ\text{C}$. Anal. ($\text{C}_{24}\text{H}_{31}\text{N}_3\text{O}_5\cdot 0.25\text{H}_2\text{O}$) C, H, N. **10c**: 93% yield. Mp: $156\text{--}58^\circ\text{C}$. Anal. ($\text{C}_{26}\text{H}_{35}\text{N}_3\text{O}_5\cdot 0.25\text{H}_2\text{O}$) C, H, N.

N-[(2R)-2-[(tert-Butoxycarbonyl)methyl]-6-hydroxyhexanoyl]-L-phenylalanine N-Methylamide (11b). A solution of **9b** (2.5 g, 0.005 mol) dissolved in absolute ethanol (50 mL) was treated with 20% palladium hydroxide on carbon (0.75 g, Degussa type) and 1,4-cyclohexadiene (4.73 mL, 0.05 mol) under a nitrogen atmosphere. The reaction mixture was warmed slowly to 65°C while stirring. The reaction mixture was stirred at 65°C until the starting material had been consumed (as followed by TLC). The reaction mixture was cooled and filtered through Celite and the Celite washed with EtOAc. The solvent was evaporated from the combined filtrates and the gummy residue purified via recrystallization

from Et₂O/hexane giving pure **11b** (1.3 g, 64% yield) as white crystals: mp 102–104 °C. ¹H-NMR (CDCl₃): δ 1.00–1.70 (m, 15H), 2.25–2.60 (m, 3H), 2.69 (d, 3H), 3.00–3.20 (m, 2H), 3.50–3.70 (m, 2H), 4.56 (q, 1H), 6.15 (m, 1H), 7.13 (d, 1H), 7.15–7.45 (m, 5H). MS: *m/z* 407 (MH⁺). Anal. (C₂₂H₃₄N₂O₅·0.25H₂O) C, H, N.

11c was synthesized in an analogous procedure and isolated as a white solid. **11c**: 76% yield. Mp: 104 °C. HRMS: *m/z* found, 421.26909 (MH⁺); C₂₃H₃₇N₂O₅ requires 421.27025.

11d was synthesized in an analogous procedure, starting from **9d**. The product was isolated via silica gel column chromatography (50–100% EtOAc/hexane) as a gum. **11d**: 71% yield. HRMS: *m/z* found, 373.26899 (MH⁺); C₁₉H₃₇N₂O₅ requires 373.27025.

N-[(2R)-2-[2'-(Hydroxyamino)-2'-oxoethyl]-6-hydroxyhexanoyl]-L-phenylalanine N-Methylamide (12b). **12b,c** were synthesized in a procedure analogous to that of **10b**. The intermediate acids of **11b** (**15**) and **11c** were isolated as the TFA esters of the alcohol: 69–76% yield. ¹H-NMR of the acid of **11b** (MeOH-*d*₄): δ 0.90–1.65 (m, 6H), 2.00–2.60 (m, 7H), 2.75 (dd, 1H), 2.90 (dd, 1H), 4.10 (t, 2H), 4.29 (q, 1H), 6.90–7.20 (m, 5H). HRMS: *m/z* found, 447.17345 (MH⁺); C₂₀H₂₆N₂O₆F₃ requires 447.17430.

Acid of **11c**: HRMS *m/z* found, 461.18995 (MH⁺); C₂₁H₂₈N₂O₆F₃ requires 461.18995. Final products were purified on preparative TLC (10% MeOH/ethyl acetate).

12b: 33% yield. Mp: 146–147 °C. ¹H-NMR (MeOH-*d*₄): δ 0.80–1.50 (m, 6H), 1.80–2.10 (m, 2H), 2.30–2.44 (m, 1H), 2.47 (s, 3H), 2.95 (dd, 1H), 2.72 (dd, 1H), 3.25 (t, 2H), 4.30 (q, 1H), 6.90–7.30 (m, 5H). HRMS: *m/z* found, 366.20254 (MH⁺); C₁₈H₂₈N₃O₅ requires 366.20290. Anal. (C₁₈H₂₇N₃O₅·CH₂Cl₂) C, H, N.

12c: 48% yield. Mp: 158–159 °C. HRMS: *m/z* found, 380.27752 (MH⁺); C₁₉H₃₀N₃O₅ requires 380.21855. Anal. (C₁₉H₂₉N₃O₅Cl·0.25CH₂Cl₂·0.25H₂O) C, H, N.

N-[(2R)-2-[tert-Butoxycarbonylmethyl]-6-phenoxyhexanoyl]-L-phenylalanine N-Methylamide (13b). Diethyl azodicarboxylate (DEAD) (0.145 mL, 0.837 mmol) was added dropwise via syringe to a solution of triphenylphosphine (0.218 g, 0.837 mmol) in dry THF (20 mL) under a nitrogen atmosphere. The mixture was stirred at room temperature for 15 min; then phenol (0.078 g, 0.837 mmol) and compound **11b** (0.340 g, 0.837 mmol) were added in one portion, and the resulting mixture was stirred at room temperature for 18 h. The solvent was evaporated and the residue dissolved in EtOAc. The EtOAc layer was washed with H₂O and brine, dried over Na₂SO₄, and filtered. The EtOAc was evaporated, the residue taken up in Et₂O/hexane, and the solution cooled over night. The precipitated reduced DEAD was filtered and washed with fresh Et₂O and the solvent evaporated from the combined filtrates. The residue was chromatographed on silica gel (30–45% EtOAc/hexane), affording **13b** (0.255 g, 63.2% yield) as a gum. ¹H-NMR (CDCl₃): δ 1.25–1.85 (m, 15H), 2.28–2.78 (m, 6H), 3.00–3.20 (m, 2H), 3.88 (t, 2H), 4.54 (dd, 1H), 5.95 (m, 1H), 6.45 (d, 1H), 6.75–7.40 (m, 10H). HRMS: *m/z* found, 483.28573 (MH⁺); C₂₈H₃₉N₂O₅ requires 483.28590.

13c-p were synthesized from **11b-d** in an analogous procedure. Except for **13c**, all were isolated as gums. **13c**: isolated as a white solid, 75% yield. Mp: 74–75 °C.

N-[(2R)-2-[2'-(Hydroxyamino)-2'-oxoethyl]-6-phenoxyhexanoyl]-L-phenylalanine N-Methylamide (14b). **14b-p** were synthesized in a procedure analogous to that of **10b**. All of the intermediate acids, excepts the acids of **13b,c,m**, were isolated as gums. Acid of **13b**: isolated as a colorless solid, 87% yield. Mp: 154 °C. ¹H-NMR (MeOH-*d*₄): δ 1.00–1.60 (m, 6H), 2.05–2.60 (m, 6H), 2.69–3.00 (2 dd, 2H), 3.66 (t, 2H), 4.30 (dd, 1H), 6.60–7.20 (m, 10H). HRMS: *m/z* found, 427.22320 (MH⁺); C₂₄H₃₁N₂O₅ requires 427.22330. Acid of **13c**: isolated as a solid, 88% yield. Mp: 151–152 °C. Acid of **13m**: isolated as a white solid, 85% yield. Mp: 138–140 °C.

14b-p were isolated as white to off-white solids. **14b**: 57% yield. Mp: 145–146 °C. ¹H-NMR (MeOH-*d*₄): δ 0.90–1.60 (m, 6H), 1.80–2.14 (2 dd, 2H), 2.32–2.54 (m, 4H), 2.54 (dd, 1H), 2.94 (dd, 1H), 3.68 (t, 2H), 4.32 (dd, 1H), 6.6–7.7 (m, 10H). HRMS: *m/z* found, 442.23452 (MH⁺); C₂₄H₃₂N₃O₅ requires

442.23420. Anal. (C₂₄H₃₁N₃O₅·0.5CH₂Cl₂·1.0H₂O) C, H, N. **14c**: 70% yield. Mp: 148–149 °C. HRMS: *m/z* found, 456.24998 (MH⁺); C₂₅H₃₅N₃O₅ requires 456.24985. Anal. (C₂₅H₃₃N₃O₅·1.75H₂O) C, H, N. **14d**: 74% yield. Mp: 180–181 °C. Anal. (C₂₁H₃₃N₃O₅·0.5H₂O) C, H, N. **14e**: 49% yield. Mp: 193 °C. Anal. (C₂₂H₃₅N₃O₅) C, H, N. **14f**: 61% yield. Mp: 81–83 °C. Anal. (C₂₄H₃₉N₃O₅·0.5H₂O) C, H, N. **14g**: 52% yield. Mp: 97–99 °C. Anal. (C₂₄H₃₉N₃O₅·0.5H₂O) C, H, N. **14h**: 67% yield. Mp: 94–96 °C. Anal. (C₂₅H₄₁N₃O₅·0.5H₂O) C, H, N. **14i**: 57% yield. Mp: 79–81 °C. Anal. (C₂₆H₄₃N₃O₅·0.5H₂O) C, H, N. **14j**: 86% yield. Mp: 179–181 °C. Anal. (C₂₁H₃₂N₃O₅·0.25H₂O) C, H, N. **14k**: 27% yield. Mp: 185–186 °C. Anal. (C₂₁H₃₂N₃O₅F) C, H, N. **14l**: 32% yield. Mp: 166–168 °C. Anal. (C₂₂H₃₅N₃O₆) C, H, N. **14m**: 29% yield. Mp: 211–213 °C. Anal. (C₂₂H₃₅N₃O₅) C, H, N. **14n**: 11% yield. Mp: 192 °C. Anal. (C₂₁H₃₂N₃O₅Cl·0.25H₂O) C, H, N. **14o**: 10% yield. Mp: 182–183 °C. Anal. (C₂₂H₃₅N₃O₆) C, H, N. **14p**: 33% yield. Mp: 171 °C. Anal. (C₂₁H₃₁N₃O₅Cl₂·H₂O) C, H, N.

N-[(2R)-2-[2'-(Phenylmethoxy)amino]-2'-oxoethyl]-6-hydroxyhexanoyl]-L-phenylalanine N-Methylamide (16). Carboxylic acid **15** (0.035 g, 0.08 mmol) was dissolved in anhydrous DMF (1 mL) and cooled to –10 °C under a nitrogen atmosphere. *N*-Methylmorpholine (0.017 mL, 0.15 mmol) followed by isobutyl chloroformate (0.02 mL, 0.15 mmol) was then added dropwise via syringe. The reaction mixture was stirred for 20 min; then a suspension of *O*-benzylhydroxylamine hydrochloride (0.024 g, 0.15 mmol) and *N*-methylmorpholine (0.017 mL, 0.15 mmol) in DMF (1.5 mL) was added dropwise via syringe. After stirring for 20 min, the reaction mixture was allowed to warm to room temperature and then stirred for 3 h. The DMF was evaporated and the residue dissolved in EtOAc. The EtOAc layer was washed with 5% citric acid, 5% NaHCO₃, H₂O, and brine, dried over Na₂SO₄, and filtered. The solvent was evaporated, and the solid residue was triturated with Et₂O and filtered, affording compound **16** (10 mg, 28%). ¹H-NMR (MeOH-*d*₄): δ 1.6–1.1 (m, 6H), 2.13 (m, 2H), 2.67 (m, 1H), 2.69 (d, 3H), 3.15 (dd, 1H), 2.94 (dd, 1H), 3.48 (t, 2H), 4.50 (m, 1H), 4.80 (s, 2H), 7.4–7.17 (m, 10H), 7.94 (m, 1H), 8.24 (d, 1H).

N-[(2R)-2-[2'-(Phenylmethoxy)amino]-2'-oxoethyl]-5-carboxypentanoyl]-L-phenylalanine N-Methylamide (17). A solution of compound **16** (0.05 g, 0.11 mmol) in DMF (1 mL) was treated with pyridinium dichromate (0.144 g, 0.38 mmol) at room temperature overnight. The reaction mixture was partitioned between EtOAc and water. The aqueous layer was separated and extracted with EtOAc. The combined EtOAc extracts were dried over Na₂SO₄ and filtered. The solvent was evaporated, and the gummy residue was triturated with Et₂O, affording **17** (0.023 g, 45% yield) as an off-white solid. ¹H-NMR (MeOH-*d*₄): δ 1.6–1.1 (m, 6H), 2.27–2.02 (m, 4H), 2.70 (m, 4H), 3.15 (dd, 1H), 2.92 (dd, 1H), 4.55 (m, 1H), 4.80 (s, 2H), 7.43–7.10 (m, 10H), 7.91 (m, 1H), 8.24 (d, 1H).

N-[(2R)-2-[2'-(Hydroxyamino)-2'-oxoethyl]-5-carboxypentanoyl]-L-phenylalanine N-Methylamide (18). Compound **17** (0.023 g, 0.049 mmol) in ethanol (5 mL) was treated with 10% Pd/C (0.010 g) and pyridine (2 drops) under a hydrogen atmosphere. The reaction mixture was stirred until the starting material was consumed (as followed by TLC). It was then filtered and the filtrate evaporated to a yellow oil. This was placed under high vacuum for several hours and then triturated with Et₂O. The solid formed was collected by filtration and dried under a nitrogen flow, affording **18** (10 mg, 54%) as an off-white solid. ¹H-NMR (MeOH-*d*₄): δ 1.91–1.35 (m, 6H), 2.30–2.10 (m, 4H), 2.62 (m, 1H), 2.70 (s, 3H), 2.95 and 3.15 (m, 4H), 4.52 (t, 1H), 7.36–7.15 (m, 5H). HRMS: *m/z* found, 380.18311 (MH⁺); C₁₈H₂₆N₃O₆ requires 380.18216.

N-[(2R)-2-[tert-Butoxycarbonylmethyl]-5-carboxypentanoyl]-L-phenylalanine N-Methylamide (19). Pyridinium dichromate (0.658 g, 1.7 mmol) was added to a solution of compound **11b** (0.203 g, 0.5 mmol) in DMF (2 mL) under a nitrogen atmosphere. The reaction mixture was stirred at room temperature for 16 h and then diluted with H₂O and extracted with EtOAc. The combined EtOAc layers were washed with H₂O and brine, dried over Na₂SO₄, and filtered.

The solvent was evaporated, and the gummy, crude product **19** (0.18 g) was used in the next step without any further purification. A small amount of pure sample was obtained via silica gel chromatography (3–15% MeOH/EtOAc) as a glass. ¹H-NMR (CDCl₃): δ 1.10–1.80 (m, 13H), 2.20–2.80 (m, 8H), 3.00–3.20 (m, 2H), 4.68 (q, 1H), 6.50 (s, 1H), 7.00–7.60 (m, 5H). MS: *m/z* 421 (MH⁺). Anal. (C₂₂H₃₂N₂O₆·0.5H₂O) C, H, N.

N-[(2R)-2-[(tert-Butoxycarbonyl)methyl]-6-(propylamino)-6-oxohexanoyl]-L-phenylalanine N-Methylamide (20a). A solution of **19** (0.18 g, 0.43 mmol) and *n*-propylamine (0.14 mL, 1.7 mmol) in dry DMF (5 mL) under nitrogen was cooled to –10 °C and treated dropwise with diethyl cyanophosphonate (0.07 mL, 0.43 mmol) followed by Et₃N (0.12 mL, 0.85 mmol). The reaction mixture was stirred at –10 °C for 1 h and then allowed to warm to room temperature over 1 h. The reaction mixture was stirred at room temperature for 3 h and then diluted with H₂O and extracted with EtOAc. The combined organic layers were washed with 5% citric acid, saturated NaHCO₃, H₂O, and brine, dried over Na₂SO₄, and filtered. The solvent was evaporated and the residue triturated with Et₂O. The solid formed was collected by filtration and air-dried to give **20a** (0.065 g) as an off-white solid. The overall yield for two steps was 28%. Mp: 155–156 °C. ¹H-NMR (CDCl₃): δ 0.91 (t, 2H), 1.30–1.80 (m, 15H), 2.13 (t, 2H), 2.25–2.60 (m, 3H), 2.71 (d, 3H), 3.05–3.30 (m, 4H), 4.62 (q, 1H), 5.98 (d, 1H), 6.38 (d, 1H), 6.70 (d, 1H), 7.10–7.40 (m, 5H). HRMS: *m/z* found, 462.29726 (MH⁺), C₂₅H₄₀N₃O₅ requires 462.29680. Anal. (C₂₅H₃₉N₃O₅) C, H, N.

20b,c were synthesized in an analogous procedure. **20b**: recrystallized from EtOAc/hexane as a white solid (43%—two steps). Mp: 142–145 °C. Anal. (C₂₉H₃₉N₃O₅·0.5H₂O) C, H, N. **20c**: recrystallized from EtOAc/hexane as a glass (48%—two steps). Anal. (C₃₀H₄₁N₃O₅·0.5H₂O) C, H, N.

N-[(2R)-2-[2'-(Hydroxyamino)-2'-oxoethyl]-6-(propylamino)-6-oxohexanoyl]-L-phenylalanine N-Methylamide (21a). **21a–c** were synthesized in a method analogous to that of **10b**. The intermediate acids were isolated. Acid of **20a**: isolated as a white solid, 85% yield. Mp: 164–165 °C. ¹H-NMR (MeOH-*d*₄): δ 0.70 (t, 2H), 1.10–1.5 (m, 6H), 1.91 (t, 2H), 2.05–2.60 (m, 6H), 2.70–3.00 (m, 4H), 4.30 (q, 1H), 6.90–7.30 (m, 5H), 7.60 (m, 1H), 8.00 (d, 1H). HRMS: *m/z* found, 406.23351 (MH⁺); C₂₁H₃₂N₃O₅ requires 406.23420. Anal. (C₂₁H₃₁N₃O₅) C, H, N. Acid of **20b**: isolated as white crystals recrystallized from CH₃CN, 79% yield. Mp: 147–149 °C. Anal. (C₂₅H₃₁N₃O₅·0.75H₂O) C, H, N. Acid of **20c**: isolated as white crystals recrystallized from CH₃CN, 58% yield. Mp: 165–166 °C. Anal. (C₂₆H₃₃N₃O₅·0.25H₂O) C, H, N.

21a: isolated as a white solid, 48% yield. Mp: 166–167 °C. ¹H-NMR (MeOH-*d*₄): δ 0.70 (t, 3H), 1.10–1.50 (m, 6H), 1.80–2.10 (m, 4H), 2.30–2.60 (m, 4H), 2.65–3.05 (m, 4H), 4.30 (d, 1H), 6.90–7.30 (m, 5H). HRMS: *m/z* found, 421.24495 (MH⁺); C₂₁H₃₃N₄O₅ requires 421.24510. Anal. (C₂₁H₃₂N₄O₅·1.1H₂O) C, H, N. **21b**: isolated as a white solid after triturations with CH₂Cl₂ and CH₃CN, 50% yield. Mp: 178–179 °C. Anal. (C₂₅H₃₂N₄O₅·0.5H₂O) C, H, N. **21c**: isolated as a white solid after trituration with hot CH₂Cl₂, 54% yield. Mp: 176–178 °C. Anal. (C₂₆H₃₄N₄O₅·1.0H₂O) C, H, N.

(4S)-4-Benzyl-3-[(2'R)-2'-[(tert-butoxycarbonyl)methyl]-6'-hydroxyhexanoyl]-2-oxazolidone (22). **22** was synthesized from compound **7b** in a procedure analogous to that of **11b**. It was isolated via recrystallization (Et₂O/hexane) as a white solid: 85% yield. Mp: 73–74 °C. ¹H-NMR (CDCl₃): δ 1.4–1.8 (m, 15H), 2.54 (dd, 1H), 2.84 (2 overlapping dd, 2H), 3.4 (dd, 1H), 3.68 (t, 2H), 4.22 (m, 3H), 4.72 (m, 1H), 7.35 (m, 5H). MS: *m/z* 406 (MH⁺). Anal. (C₂₂H₃₁NO₆) C, H, N.

(4S)-4-Benzyl-3-[(2'-[(tert-butoxycarbonyl)methyl]-6'-[(methylsulfonyl)oxy]hexanoyl]-2-oxazolidone (23). Compound **22** (0.5 g, 1.23 mmol), Et₃N (0.24 mL, 1.72 mmol), and 4-(dimethylamino)pyridine (0.03 g, 0.246 mmol) were dissolved in dry CH₂Cl₂ (10 mL) and cooled to 0 °C under nitrogen. Methanesulfonyl chloride (0.105 mL, 1.35 mmol) was then added dropwise via syringe with stirring. The cloudy white reaction mixture was stirred at 0 °C for 2 h and then warmed to room temperature and the reaction quenched with H₂O. The layers were separated, and the organic layer was washed with

5% NaHCO₃, 5% citric acid, H₂O, and brine, dried over Na₂SO₄, and filtered. Evaporation of the solvent afforded **23** (0.57 g, 96%) as a colorless oil, which was used without further purification. ¹H-NMR (CDCl₃): δ 1.41–1.84 (m, 15H), 2.48 (dd, 1H), 2.84 (overlapping dd, 2H), 3.02 (s, 3H), 3.34 (dd, 1H), 4.13–4.28 (m, 5H), 4.69 (m, 1H), 7.23–7.39 (m, 5H).

(4S)-4-Benzyl-3-[(2'R)-2'-[(tert-butoxycarbonyl)methyl]-6'-azidohexanoyl]-2-oxazolidone (24). Compound **23** (2.1 g, 4.34 mmol) and tetrabutylammonium iodide (1.6 g, 4.34 mmol) were dissolved in toluene (20 mL). A sodium azide solution (2.8 g, 43 mmol) in H₂O (20 mL) was then added in one portion and the two-phase reaction mixture stirred vigorously at 70 °C for 17 h under nitrogen. The reaction mixture was cooled, the layers were separated, and the aqueous layer was extracted with EtOAc. The EtOAc and toluene layers were combined and washed with 5% NaHCO₃, 5% citric acid, H₂O, and brine and then dried over Na₂SO₄ and filtered. The solvent was evaporated, leaving an oil residue which solidified. The solid was recrystallized from hexane, affording **24** (1.5 g, 80%) as colorless crystals: mp 92 °C. ¹H-NMR (CDCl₃): δ 1.45–1.75 (m, 15H), 2.47 (dd, 1H), 2.78 (2 overlapping dd, 2H), 3.28 (t, 2H), 3.34 (dd, 1H), 4.17 (m, 3H), 4.67 (m, 1H), 7.23–7.37 (m, 5H). Anal. (C₂₂H₃₀N₄O₅) C, H, N.

(2R)-2-[(tert-Butoxycarbonyl)methyl]-6-azidohexanoic acid (25). Compound **25** was synthesized in a procedure analogous to that of **8b** and isolated as a colorless oil: 90% yield. ¹H-NMR (CDCl₃): δ 1.39–1.7 (m, 15H), 2.4 (dd, 1H), 2.65 (dd, 2H), 2.82 (m, 1H), 3.29 (t, 2H). Anal. (C₁₂H₂₁N₃O₄) C, H, N.

N-[(2R)-2-[(tert-Butoxycarbonyl)methyl]-6-azidohexanoyl]-L-phenylalanine N-Methylamide (26). Compound **26** was synthesized in a procedure analogous to that of **9b**. The product was isolated as a solid and recrystallized in Et₂O/hexane, affording **26** as a white solid: 74% yield. Mp: 99–100 °C. ¹H-NMR (CDCl₃): δ 1.4–1.68 (m, 15H), 2.3–2.58 (m, 3H), 2.7 (d, 3H), 3.09 (2 dd, 2H), 3.21 (t, 2H), 4.51 (q, 1H), 5.81 (d, 1H), 6.35 (d, 1H), 7.19–7.33 (m, 5H). Anal. (C₂₂H₃₃N₅O₄) C, H, N.

N-[(2R)-2-[(tert-Butoxycarbonyl)methyl]-6-[4'-oxobutylamino]hexanoyl]-L-phenylalanine N-Methylamide (27). Compound **26** (0.083 g, 0.19 mmol) in dry/distilled THF (15 mL) was hydrogenated (0.1 g of 10% Pd/C, 30 psi, 25 °C, 1.2 h) on a Parr shaker apparatus. After this time, the reaction mixture was filtered through Celite and the Celite washed with EtOH. The combined filtrates were evaporated, affording the amine intermediate (0.084 g, 90%) as a gum. ¹H-NMR (MeOH-*d*₄): δ 1.1–1.5 (m, 15H), 2.15–2.41 (m, 3H), 2.47–2.61 (m, 5H), 2.9 (dd, 1H), 3.05 (dd, 1H), 4.41 (t, 1H), 7.07–7.26 (m, 5H).

The crude amine (0.394 g, 0.97 mmol) was dissolved in dry DMF (15 mL) and cooled to –10 °C under a nitrogen atmosphere. Et₃N (0.203 mL, 1.46 mmol) followed by butyryl chloride (0.111 mL, 1.07 mmol) was added dropwise via syringe. The cloudy white reaction mixture was stirred for 20 min at –10 °C and then warmed to room temperature and stirred for 1.5 h. The DMF was evaporated and the residue taken into EtOAc. The EtOAc layer was washed with 5% NaHCO₃, 5% citric acid, H₂O, and brine, dried over Na₂SO₄, and filtered. The solvent was evaporated, and the solid residue was recrystallized in CH₃CN/Et₂O and washed with cold Et₂O, affording **27** (0.29 g, 63%) as a white solid: mp 160–161 °C. ¹H-NMR (CDCl₃): δ 0.95 (t, 3H), 1.2–1.71 (m, 17H), 2.15 (t, 2H), 2.27–2.59 (m, 3H), 2.7 (d, 3H), 3.09 (2 dd, 2H), 3.21 (m, 2H), 4.51 (q, 1H), 5.81 (br s, 1H), 5.89 (br s, 1H), 6.35 (d, 1H), 7.14–7.34 (m, 5H). Anal. (C₂₆H₄₁N₃O₅·0.25H₂O) C, H, N.

N-[(2R)-2-[2'-(Hydroxyamino)-2'-oxoethyl]-6-[4'-oxobutylamino]hexanoyl]-L-phenylalanine N-Methylamide (29). Compound **29** was synthesized from **27** in a procedure analogous to that of **10b**. **28**: isolated as a white powder after trituration with Et₂O, 94% yield. Mp: 182–183 °C. ¹H-NMR (MeOH-*d*₄): δ 0.87 (t, 3H), 1.02–1.63 (m, 8H), 2.08 (t, 2H), 2.2–2.48 (2 dd, 2H), 2.56 (m, 4H), 2.84–3.1 (m, 4H), 4.41 (t, 1H), 7.02–7.27 (m, 5H). MS: *m/z* 420 (MH⁺). Anal. (C₂₂H₃₃N₃O₅·0.5H₂O) C, H, N.

29: isolated as a white powder after trituration with Et₂O, 78% yield. Mp: 186 °C. ¹H-NMR (MeOH-*d*₄): δ 0.85 (t, 2H),

0.99–1.61 (m, 8H), 1.98–2.2 (m, 4H), 2.48–2.63 (m, 4H), 2.81–3.11 (m, 4H), 4.41 (q, 1H), 7.13–7.25 (m, 5H). MS: m/z 435 (MH⁺). Anal. (C₂₂H₃₄N₄O₅) C, H, N.

(4S)-4-Benzyl-3-[(2R)-2'-(tert-butoxycarbonyl)methyl]-6'-(4-chlorophenoxy)hexanoyl]-2-oxazolidone (30). Compound **30** was synthesized in a procedure analogous to that of **13b** and isolated as a white solid after silica gel column chromatography (10–20% EtOAc/hexane): 75% yield. Mp: 84–85 °C. ¹H-NMR (CDCl₃): δ 1.42 (s, 9H), 2.54 (m, 3H), 2.77 (m, 3H), 2.48 (dd, 1H), 2.78 (m, 2H), 3.33 (dd, 1H), 3.90 (t, 2H), 4.15 (m, 3H), 4.67 (m, 1H), 6.80 (d, 2H), 7.27 (m, 7H). HRMS: m/z found, 515.20717 (MH⁺); C₂₈H₃₄NO₆Cl requires 515.20747. Anal. (C₂₈H₃₃NO₆Cl) C, H, N, Cl.

(2R)-2-[(tert-Butoxycarbonyl)methyl]-6-(4-chlorophenoxy)hexanoic Acid (31). Compound **31** was synthesized in a procedure analogous to that of **8b**: 73% yield. Mp: 83–84.5 °C. ¹H-NMR (CDCl₃): δ 1.41 (s, 9H), 1.53 (m, 3H), 1.76 (m, 3H), 2.40 (dd, 1H), 2.62 (dd, 1H), 2.83 (m, 1H), 2.90 (t, 2H), 6.80 (d, 2H), 7.20 (d, 2H). Anal. (C₁₈H₂₅O₅Cl) C, H, Cl.

(2S)-2-[N-[(2R)-2'-(tert-Butoxycarbonyl)methyl]-6'-(4-chlorophenoxy)hexanoyl]amino]-3,3-dimethylbutanoic Acid N-(1-Pyrrolidinoethyl)amide (33a). Compounds **33a–g** were prepared in a method analogous to that of **9b**. **33a**: 87% yield. ¹H-NMR (CDCl₃): δ 0.96 (s, 9H), 1.42–1.51 (m, 12H), 1.74 (m, 3H), 2.36 (dd, 1H), 2.6 (m, 4H), 3.51 (dd, 2H), 3.87 (t, 2H), 4.2 (d, 1H), 5.12 (s, 2H), 6.42 (t, 1H), 6.51 (d, 1H), 6.8 (d, 2H), 7.2 (d, 2H), 7.36 (m, 5H). HRMS: m/z found, 631.31405 (MH⁺); C₃₄H₄₈N₂O₇Cl requires 631.31501. Anal. (C₃₄H₄₇N₂O₇Cl) C, H, N.

(2S)-2-[N-[(2R)-2'-[2''-(Hydroxyamino)-2''-oxoethyl]-6'-(4-chlorophenoxy)hexanoyl]amino]-3,3-dimethylbutanoic Acid N-(1-Pyrrolidinoethyl)amide (34a). Compounds **34a–e** were synthesized in a procedure analogous to that of **10b**. **34a**: 57% yield. Mp: 105–109 °C. ¹H-NMR (DMSO-*d*₆): δ 0.92 (s, 9H), 1.28–2.25 (m, 13H), 2.8–3.23 (m, 6H), 3.35–3.55 (m, 3H), 3.90 (t, 2H), 4.18 (d, 1H), 6.94 (d, 2H), 7.32 (d, 2H), 7.88 (d, 1H), 8.32 (m, 1H). HRMS: m/z found, 525.28403 (MH⁺); C₂₆H₄₂N₄O₅Cl requires 525.28437. **34b**: 34% yield. HRMS: m/z found, 555.29533 (MH⁺); C₂₇H₄₄N₄O₆Cl requires 555.29494. **34c**: 56% yield. Mp: 104–105 °C. Anal. (C₂₈H₃₉N₄O₇Cl·0.5H₂O) C, H, N. **34d**: 72% yield. Mp: 74–75 °C. Anal. (C₂₈H₃₈N₃O₅Cl·0.5H₂O) C, H, N. **34e**: 21% yield. HRMS: m/z found, 533.25344 (MH⁺); C₂₇H₃₈N₄O₅Cl requires 533.25307.

(2S)-2-[N-[(2R)-2'-[2''-(Hydroxyamino)-2''-oxoethyl]-6'-phenoxyhexanoyl]amino]-3,3-dimethylbutanoic Acid N-(2-Carboxyethyl)amide (34f). Compound **34f** (2.27 g, 3.81 mmol) was dissolved in CH₂Cl₂ (40 mL) and cooled in an ice bath. The reaction mixture was treated with TFA (7 mL) and allowed to stir while warming to room temperature until the ester was consumed (as followed by TLC). The CH₂Cl₂ and excess TFA were evaporated, and the gummy residue was placed under high vacuum overnight. It was then purified via silica gel column chromatography (25–60% EtOAc/hexane) which afforded the acid of **34f** (1.38 g, 63%) as a white foam. ¹H-NMR (CDCl₃): δ 0.97 (s, 9H), 1.35–1.84 (m, 6H), 2.48–2.65 (m, 3H), 2.76–2.91 (m, 2H), 3.42–3.69 (m, 2H), 3.88 (t, 2H), 4.39 (d, 1H), 5.16 (s, 2H), 6.84 (m, 3H), 7.22 (d, 2H), 7.4 (m, 6H). HRMS: m/z found, 575.25296 (MH⁺); C₃₀H₄₀N₂O₇Cl requires 575.25240.

The acid of **34f** (1.24 g, 2.15 mmol) was converted to its corresponding *O*-benzyl hydroxamate by treating it with DEPC (0.36 mL, 2.15 mmol) and *O*-benzylhydroxylamine hydrochloride (0.38 g, 2.37 mmol) in anhydrous DMF (30 mL). The reaction mixture was cooled to –10 °C under a nitrogen atmosphere; then Et₃N (0.75 mL, 5.39 mmol) was added dropwise via syringe. The reaction mixture was allowed to stir overnight while warming to room temperature. The DMF was evaporated, and the residue was partitioned between H₂O and EtOAc. The separated EtOAc layer was washed with H₂O several times and then with brine, dried over Na₂SO₄, and filtered. The solvent was evaporated and the residue purified via silica gel column chromatography (25–90% EtOAc/hexane), affording the *O*-benzyl hydroxamate of **34f** (1.1 g, 75%) as a white foam. ¹H-NMR (CDCl₃): δ 0.96 (s, 9H), 1.32–1.78 (m,

6H), 2.19 (dd, 1H), 2.41–2.72 (m, 3H), 3.05–3.31 (m, 2H), 3.61 (m, 1H), 3.83 (t, 2H), 4.5 (d, 1H), 4.88 (s, 2H), 5.08 (s, 2H), 6.78 (d, 2H), 7.00 (br d, 1H), 7.2 (d, 2H), 7.36 (m, 10H), 7.6 (br s, 1H), 9.65 (br s; 1H). HRMS: m/z found, 680.31254 (MH⁺); C₃₇H₄₇N₃O₇Cl requires 680.31025.

The *O*-benzyl hydroxamate of **33g** was synthesized in a similar manner to **34f** and isolated as a gum in 79% yield. HRMS: m/z found, 694.32564 (MH⁺); C₃₈H₄₉N₃O₇Cl requires 694.32590.

Hydroxamates **34f,g** were prepared from their corresponding *O*-benzyl hydroxamates in a procedure analogous to that of compound **18** and isolated as glasses via silica gel chromatography (75–100% EtOAc/hexane and then 5–20% MeOH/EtOAc). **34f**: 21% yield. ¹H-NMR (MeOH-*d*₄): δ 0.9 (s, 9H), 1.25–1.72 (m, 6H), 2.19 (dd, 2H), 2.35 (t, 2H), 2.78 (m, 1H), 3.17–3.4 (m, 2H), 3.81 (t, 2H), 4.11 (s, 1H), 6.77 (t, 3H), 7.11 (t, 2H). HRMS: m/z found, 466.25456 (MH⁺); C₂₃H₃₆N₃O₇ requires 466.25533. **34g**: 33% yield. HRMS: m/z found, 480.27006 (MH⁺); C₂₄H₃₈N₃O₇ requires 480.27098.

Acknowledgment. The assistance of Mr. Travis Stams and Ms. Angela Smallwood for crystallization trials and data analysis, Ms. Tammi Yacobucci and Mr. Brent Douty for chemical intermediates, and Mr. Al Hlavac for mass spectral data is greatly appreciated.

References

- (1) Birkedal-Hansen, H.; Moore, W. G. I.; Bodden, M. K.; Windsor, L. J.; Birkedal-Hansen, B.; DeCarlo, A.; Engler, J. A. Matrix Metalloproteinases: A Review. *Crit. Rev. Oral Biol. Med.* **1993**, *4*, 197–250.
- (2) Walakovits, L. A.; Bhardwaj, N.; Gallick, G. S.; Lark, M. W. Detection of High Levels of Stromelysin and Collagenase in Synovial Fluid from Patients with Rheumatoid Arthritis and Post-Traumatic Knee Injury. *Arthritis Rheum.* **1992**, *35*, 35–42.
- (3) Pyke, C.; Ralfkiaer, E.; Huhtala, P.; Hurskaia, T.; Dano, K.; Tryggvason, K. Localization of Messenger RNA for M_r 72,000 and 92,000 Type IV Collagenases in Human Skin Cancers by *in situ* Hybridization. *Cancer Res.* **1992**, *52*, 1336–1341.
- (4) Overall, C. M.; Wiebkin, O. W.; Thonard, J. C. Demonstration of Tissue Collagenase Activity *in vivo* and its Relationship to Inflammation Severity in Human Gingiva. *J. Periodontol Res.* **1987**, *22*, 81–88.
- (5) Burns, F. R.; Stack, M. S.; Gray, D.; Paterson, C. A. Inhibition of Purified Collagenase from Alkali-burned Rabbit Corneas. *Invest. Ophthalmol. Visual Sci.* **1989**, *32*, 1569–1575.
- (6) Gijbels, K.; Masure, S.; Carton, H.; Opendakker, G. Gelatinase in the Cerebrospinal Fluid of Patients with Multiple Sclerosis and other Inflammatory Neurological Disorders. *J. Neuroimmunol.* **1992**, *41*, 29–34.
- (7) Henney, A. M.; Wakeley, P. R.; Davies, M. J.; Foster, K.; Hembry, R.; Murphy, G.; Humphries, S. Localization of stromelysin gene expression in atherosclerotic plaques by *in situ* hybridization. *Proc. Natl. Acad. Sci. U.S.A.* **1991**, *88*, 8154–8158.
- (8) Vine, N.; Powell, J. T. Metalloproteinases in Degenerative Aortic Diseases. *Clin. Sci.* **1991**, *81*, 233–239.
- (9) Kronberger, A.; Valle, K. J.; Eisen, A. Z.; Bauer, E. A. Enhanced Cell-free Translation of Human Skin Collagenase in Recessive Dystrophic Epidermolysis Bullosa. *J. Invest. Dermatol.* **1982**, *79*, 208–211.
- (10) Sawamura, D.; Sawamura, T.; Hashimoto, I.; Bruckmer-Tuderman, L.; Fujimoto, D.; Okada, Y.; Utsumi, N.; Shikata, H. Increased Gene Expression of Matrix Metalloproteinase-3 (Stromelysin) in Skin Fibroblasts from Patients with Severe Recessive Dystrophic Epidermolysis Bullosa. *Biochem. Biophys. Res. Commun.* **1991**, *174*, 1003–1008.
- (11) Winyard, P. G.; Zhang, Z.; Chidwick, K.; Blake, D. R.; Carrell, R. W.; Murphy, G. Proteolytic Inactivation of Human α₁-Antitrypsin by Human Stromelysin. *FEBS Lett.* **1991**, *279*, 91–94.
- (12) Johnson, W. H.; Roberts, N. A.; Borkakoti, N. Collagenase Inhibitors: Their Design and Potential Therapeutic Use. *J. Enzyme Inhib.* **1987**, *2*, 1–22.
- (13) Wahl, R. C.; Dunlap, R. P.; Morgan, B. A. Biochemistry and Inhibition of Collagenase and Stromelysin. *Annu. Rep. Med. Chem.* **1990**, *25*, 177–184.
- (14) Henderson, B.; Docherty, A. J. P.; Beeley, N. R. A. Design of Inhibitors of Articular Cartilage Destruction. *Drugs Future* **1990**, *15*, 495–508.
- (15) Beeley, N. R. A.; Ansell, P. R. J.; Docherty, A. J. P. Inhibitors of Matrix Metalloproteinases (MMP's). *Curr. Opin. Ther. Patents* **1994**, *4*, 7–16.

- (16) Schwartz, M. A.; VanWart, H. E. In *Progress in Medicinal Chemistry: Volume 29*; Ellis, G. P., Luscomb, D. K., Eds.; Elsevier Science Publishers: London, 1992; Chapter 8.
- (17) Davies, B.; Brown, P. D.; East, N.; Crimmin, M. J.; Balkwill, F. R. A Synthetic Matrix Metalloproteinase Inhibitor decreases Tumor Burden and Prolongs Survival of Mice Bearing Human Ovarian Carcinoma Xenografts. *Cancer Res.* **1993**, *53*, 2087-2091.
- (18) *Ophthalmology Times* **1992**, Nov. 15, 9.
- (19) Lewis, E. J.; Bottomley, K. M. K.; Broadhurst, M. J.; Brown, P. A.; Hallam, T. J.; Johnson, W. H.; Lawton, G.; Nixon, J. S. Orally Active Inhibitors of Collagen Degradation. Presented at Joint BCTS and BCR Meeting, Cambridge, U.K., 1993.
- (20) Spurlino, J. C.; Smallwood, A. M.; Carlton, D. D.; Banks, T. M.; Vavra, K. J.; Johnson, J. S.; Cook, E. R.; Falvo, J.; Wahl, R. C.; Pulvino, T. A.; Wendoloski, J. J.; Smith, D. L. 1.56 Å Structure of Mature Truncated Human Fibroblast Collagenase. *Proteins: Struct., Funct., Genet.* **1994**, *19*, 98-109.
- (21) Stams, T.; Spurlino, J. C.; Smith, D. L.; Wahl, R. C.; Ho, T. F.; Qoronfleh, M. W.; Banks, T. M.; Rubin, B. Structure of Human Neutrophil Collagenase Reveals Large S₁' Specificity Pocket. *Nature: Struct. Biol.* **1994**, *1*, 119-123.
- (22) Lovejoy, B.; Cleasby, A.; Hassell, A. M.; Longley, K.; Luther, M. A.; Weigl, D.; McGeehan, G.; McElroy, A. B.; Drewry, D.; Lambert, M. H.; Jordan, S. R. Structure of the Catalytic Domain of Fibroblast Collagenase Complexed with an Inhibitor. *Science* **1993**, *263*, 275-277.
- (23) Borkakoti, N.; Winkler, F. K.; Williams, D. H.; D'Arcy, A.; Broadhurst, M. J.; Brown, P. A.; Johnson, W. H.; Murray, E. J. Structure of the Catalytic Domain of Fibroblast Collagenase Complexed with an Inhibitor. *Nature: Struct. Biol.* **1994**, *1*, 106-110.
- (24) Mathiowetz, A. M. Unpublished results.
- (25) Tomczuk, B. E.; Gowravaram, M. R.; Johnson, J. S.; Delecki, D.; Cook, E. R.; Ghose, A. K.; Mathiowetz, A. M.; Spurlino, J. C.; Rubin, B.; Smith, D. L.; Pulvino, T.; Wahl, R. C. Hydroxamate Inhibitors of the Matrix Metalloproteinases (MMPs) containing Novel P₁' Heteroatom Based Modifications. *BioMed. Chem. Lett.* **1995**, *5*, 343-348.
- (26) Broadhurst, M. J.; Brown, P. A.; Johnson, W. H.; Lawton, G. *Eur. Pat. Appl.* 0497192A2, 1992.
- (27) The inhibitory potencies against the truncated enzymes were identical to the potencies against the mature full-length enzymes for a select group of compounds in Tables 1-3 (data not shown).
- (28) Wolfenden, R. Interaction of the Peptide Bond with Solvent Water: A Vapor Phase Analysis. *Biochemistry* **1978**, *17*, 201-204.
- (29) Tanford, C. *The Hydrophobic Effect*; Wiley: New York, 1974.
- (30) Flocco, M. M.; Mowbray, S. L. Planar Stacking Interactions of Arginine and Aromatic Side-Chains in Proteins. *J. Mol. Biol.* **1994**, *235*, 709-717.
- (31) Liu, S.; Ji, X.; Gilliland, G. L.; Stevens, W. J.; Armstrong, R. N. Second-Sphere Electrostatic Effects in the Active Site of Glutathione S-Transferase. Observation of an On-Face Hydrogen Bond between the Side Chain of Threonine 13 and the p-Cloud of Tyrosine 6 and Its Influence on Catalysis. *J. Am. Chem. Soc.* **1993**, *115*, 7910-7911.
- (32) Ghose, A. K. Unpublished results.
- (33) Brian, W. Unpublished results.
- (34) Goldberg, G. I.; Wilhelm, S. M.; Kronberger, A.; Bauer, E. A.; Grant, G. A.; Eisen, A. Z. Human Fibroblast Collagenase: Complete Primary Structure and Homology to an Oncogene Transformation-induced Rat Protein. *J. Biol. Chem.* **1986**, *261*, 6600-6605.
- (35) Devarajan, P. I.; Mooktiar, K.; VanWart, H. E.; Berliner, N. Structure and Expression of the cDNA encoding Human Neutrophil Collagenase. *Blood* **1991**, *77*, 2731-2738.
- (36) Ho, T. F.; Qoronfleh, M. W.; Wahl, R. C.; Pulvino, T. A.; Vavra, K. J.; Falvo, J.; Banks, T. M.; Brake, P. G.; Ciccarelli, R. B. Gene Expression, Purification, and Characterization of Recombinant Human Neutrophil Collagenase. *Gene*, in press.
- (37) Mach, H.; Middaugh, C. R.; Lewis, R. V. Statistical Determination of the Average Values of the Extinction Coefficients of Tryptophan and Tyrosine in Native Proteins. *Anal. Biochem.* **1992**, *200*, 74-80.
- (38) Moore, W. M.; Spilburg, C. A. Purification of Human Collagenases with a Hydroxamic Acid Affinity Column. *Biochemistry* **1986**, *25*, 5189-5195.

JM940720E